RL-TR-95-169
Final Technical Report
September 1995

# ULTRA-HIGH SPEED OPTICAL COMMUNICATION AND SWITCHING VIA NOVEL QUANTUM DEVICES

Northwestern University

Sponsored by
Advanced Research Projects Agency
ARPA Order No. 8544


*APPROVED FOR PUBLIC RELEASE; DISTRIBUTION UNLIMITED.*







Rome Laboratory
Air Force Materiel Command
Griffiss Air Force Base, New York

This report has been reviewed by the Rome Laboratory Public Affairs Office (PA) and is releasable to the National Technical Information Service (NTIS). At NTIS it will be releasable to the general public, including foreign nations.

RL-TR-95-169 has been reviewed and is approved for publication.

APPROVED: Paul L. Repak

PAUL L. REPAK
Project Engineer

FOR THE COMMANDER: Donald W. Hanson

DONALD W. HANSON
Director of Surveillance & Photonics

If your address has changed or if you wish to be removed from the Rome Laboratory mailing list, or if the addressee is no longer employed by your organization, please notify RL ( OCPC ) Griffiss AFB NY 13441. This will assist us in maintaining a current mailing list.

Do not return copies of this report unless contractual obligations or notices on a specific document require that it be returned.

# ULTRA-HIGH SPEED OPTICAL COMMUNICATION AND SWITCHING VIA NOVEL QUANTUM DEVICES

Horace P. Yuen
Prem Kumar
Sen-Tiong Ho

Contractor: Northwestern University
Contract Number: F30602-92-C-0086
Effective Date of Contract: 18 May 1992
Contract Expiration Date: 30 September 1994
Short Title of Work: Ultra-High Speed Optical Communication and Switching Via Novel Quantum Devices
Period of Work Covered: May 92 - Sep 94

Principal Investigator: Horace P. Yuen
Phone: (708) 491-4128

RL Project Engineer: Paul L. Repak
Phone: (315) 330-3146



This research was supported by the Advanced Research Projects Agency of the Department of Defense and was monitored by Paul L. Repak, RL (OCPC), 25 Electronic Pky, Griffiss AFB Ny 13441-4515.

# REPORT DOCUMENTATION PAGE

Form Approved
OMB No. 0704-0188



| 1. AGENCY USE ONLY (Leave Blank) | 2. REPORT DATE | 3. REPORT TYPE AND DATES COVERED |
|---|---|---|
| | September 1995 | Final May 92 - Sep 94 |

**4. TITLE AND SUBTITLE**

ULTRA-HIGH SPEED OPTICAL COMMUNICATION AND SWITCHING VIA NOVEL QUANTUM DEVICES

**5. FUNDING NUMBERS**

C - F30602-92-C-0086
PE - 62702E
PR - H544
TA - 00
WU - 01

**6. AUTHOR(S)**

Horace P. Yuen, Prem Kumar, and Seng-Tiong Ho

**7. PERFORMING ORGANIZATION NAME(S) AND ADDRESS(ES)**

Northwestern University
Dept. of Electrical Engineering & Computer Science
633 Clark St
Evanston IL 60208-1110

**8. PERFORMING ORGANIZATION REPORT NUMBER**

N/A

**9. SPONSORING/MONITORING AGENCY NAME(S) AND ADDRESS(ES)**

Advanced Research Projects Agency
3701 North Fairfax Drive
Arlington VA 22203-1714

Rome Laboratory (OCPC)
25 Electronic Pky
Griffiss AFB NY 13441-4515

**10. SPONSORING/MONITORING AGENCY REPORT NUMBER**

RL-TR-95-169

**11. SUPPLEMENTARY NOTES**

Rome Laboratory Project Engineer: Paul L. Repak/OCPC/(315) 330-3146

**12a. DISTRIBUTION/AVAILABILITY STATEMENT**

Approved for public release; distribution unlimited.

**12b. DISTRIBUTION CODE**

**13. ABSTRACT** (Maximum 200 words)

A joint theoretical-experimental research program was undertaken to initiate the development of novel quantum devices for greatly improved optical communication and switching in both local network and long haul applications. Specifically, Northwest University theoretically investigated and experimentally realized novel quantum amplifiers (phase sensitive linear amplifiers and photon number amplifiers) and ultrafast all-optical switches that would lead to the development of ultra-high speed networks. The main effort was directed toward the development of phase-sensitive switches, a preliminary experimental investigation of waveguide single-quadrature duplicator, and the corresponding theoretical support and exploration.

**14. SUBJECT TERMS**

Optical networks, Optical communications, Optical switches

**15. NUMBER OF PAGES**

64

**16. PRICE CODE**

| 17. SECURITY CLASSIFICATION OF REPORT | 18. SECURITY CLASSIFICATION OF THIS PAGE | 19. SECURITY CLASSIFICATION OF ABSTRACT | 20. LIMITATION OF ABSTRACT |
|---|---|---|---|
| UNCLASSIFIED | UNCLASSIFIED | UNCLASSIFIED | SAR |

# Contents


**1 Introduction** **5**

**2 Glossary** **7**

**3 Proposed Goals and Summary of Research Performed** **8**

3.A Analysis of Device and System Performance . . . . . 8

3.B Phase-Sensitive Amplification and Duplication of Solitons . . . . . 8

3.B.1 Phase-Sensitive Amplification of Solitons . . . . . 9

3.B.2 Photon Duplication of Solitons . . . . . 9

3.C Ultra-Fast All-Optical Switch, Gap Soliton, and Single-Quadrature Duplicator . . . . . 10

3.C.1 Compact Ultrafast All-Optical Switch . . . . . 10

3.C.2 Improved Ultrafast All-Optical Switch with Gap Soliton Propagation 10

3.C.3 Single-Quadrature Duplicator . . . . . 11

**4 Details of Research Performed and Outcomes** **12**

4.A Analysis of Device and System Performance . . . . . 12

4.A.1 Performance of Systems that Utilize Novel Quantum Devices . . . . . 12

4.A.1 Physics of the Novel Quantum Devices . . . . . 14

4.A.2 Ultimate Quantum Limit Performance Study . . . . . 14

4.B Phase-Sensitive Amplification and Duplication of Solitons . . . . . 14

4.B.1 Phase-Sensitive Amplification of Solitons . . . . . 15

4.B.2 Solitons in fiber lines with PSA's . . . . . 15

4.B.3 Dispersion compensation with PSA's . . . . . 18

4.B.4 Fiber PSA's . . . . . 21

4.B.5 Storage of soliton bit streams using PSA's . . . . . 25

4.B.6 Photon Duplication of Solitons . . . . . 26

4.C Ultra-Fast All-Optical Switch, Gap Soliton, and Single-Quadrature Duplicator . . . . . 26

4.C.1 Compact Ultrafast All-Optical Switch . . . . . 26

4.C.2 Improved Ultrafast All-Optical Switch with Gap Soliton Propagation 32

4.C.3 Single-Quadrature Duplicator . . . . . 35

**5 References** **40**

**6 List of Journal Publications Resulting from this Contract** **45**

**7 List of Conference Presentations Resulting from this Contract** **47**

# List of Figures


1 Error exponents per signal photon as a function of number of amplifier stages with gain G=10; $g_1$ applies to a PNA line and $g_2$ to a PIA line under the Gaussian approximation. . . . . 13

2 Schematic of a nonlinear optical fiber transmission line in which loss is balanced by a chain of periodically-spaced, phase-sensitive amplifiers (PSA's). . 16

3 Evolution of initial pulses $U(T,0) = \operatorname{sech} T$, (left), and $U(T,0) = 1.8 \operatorname{sech} T$, (right), showing exponential decay onto the stable pulse solution of the fiber-PSA line. . . . . 17

4 Initial pulse amplitudes $A$ and widths $T_0$ which give stable pulse solutions. The initial conditions $U(T,0) = A \operatorname{sech}(T/T_0)$, with different values of $A$ and $T_0$, were used. For all initial conditions within the lined region the same final steady-state was reached. . . . . 17

5 Magnitude of a Gaussian input pulse (dashed curves) propagating through the fiber/PSA line with $\ell = 0.08$ [plots (a) through (c)] and $\ell = 0.2$ [plots (d) through (f)]. Here $\ell$ is the ratio of the amplifier spacing to the dispersion length. In each plot the thick solid curve shows the pulse at the output of the $n$th amplifier with $n$ as indicated in the plots and the thin solid curve shows the pulse that would result if phase-insensitive amplifiers (such as EDFA's for the 1.55 $\mu$m link) are used. In plots (a) through (c) the amplifier spacing is 2.4 km and in plots (d) through (f) it is 40 km. . . . . 19

6 Schematic diagram of the 1.5 $\mu$m picosecond-pulse fiber PSA. . . . . 22

7 Phase dependence of the signal amplification for $I_s$=40 $\mu$W and $I_p$=2 mW. . 23

8 Phase-sensitive amplification of 8.3 ps pulses at 1.5 $\mu$m. The signals were monitored using a 45 GHz photodiode and a 50 GHz sampling oscilloscope. . 24

9 Maximum gain as a function of the average pump power. The squares are the data points whereas the solid curve shows the theoretically expected gain. . . 24

10 Left – Schematic of a fiber ring in which loss is compensated by phase-sensitive amplification. Right – A physically realizable optical storage ring using a fiber PSA [41]. Note that the storage ring can be loaded without keeping track of the optical phase of the data stream on the network. . . . . 25

11 SEM picture of the microfabricated strongly-guided AlGaAs waveguide. . . 28

12 Experimental set up of the Mach-Zehnder configuration for all-optical switching using AlGaAs waveguides. . . . . 29

13 The botton trace (solid curve) shows the modulated output signal at port A of the switch as function of time, while the top trace (dotted line) shows the pump on and off. When the pump is on the output signal increases showing the signal being switched from output port A to B. . . . . 30
14 Experimental set up for measuring the Bragg reflector bandwidth. . . . . 33
15 Reflectivity espectrum as function of wavelength for: (a) 1.2$\mu$m thick Bragg reflector waveguide, and (b) 1.0 $\mu$m thick Bragg reflector waveguide. . . . . 34
16 The effect of nonlinear pump-probe phase mismatch $\Delta\kappa$ on the amount of squeezing, as function of waveguide length for a square pump pulse, uniform phase LO and without nonlinear absorption: (a) $\Delta\kappa \neq 0$, and (b) $\Delta\kappa=0$. . . 36
17 Effect of SSD phase mismatch on squeezing for a Gaussian pump pulse with uniform phase under its pulse profile and without nonlinear absorptio: (a) LO pulse has the same width as the Gaussian pump pulse; (b), (c), and (d) narrow uniform-phase LO pulse, where the LO pulse width is taken to be 1/2, 1/4, and 1/8 of that of the pump pulse, respectively. Curve (e) illustrates the square pump pulse case as a comparison. . . . . 37
18 Squeezing with nonlinear absorption: (a) Gaussian pump pulse with nearly matched LO pulse from another waveguide; (b) Gaussian pump pulse with reused pump pulse; (c) Gaussian pump pulse with narrower uniform-phase LO pulse; (d) Gaussian pump pulse with uniform-phase LO having the same width as the pump; (e) Square pump pulse; (f) Relative pump amplitude $E_p(l)/E_p(0)$. . . . . 38

# 1 Introduction

A 2.5-year research program was undertaken with the main objective to initiate the development of novel quantum devices for greatly improved fiber-optic communications in both local network and long haul applications, systems that actually approach the theoretical limits consistent with communication theory and the laws of physics. As part of the program, novel devices involving gap solitons were also studied for high-speed optical switching, which are generally applicable to optical computing as well as communication systems.

Long haul fiber optical communication is presently limited by loss and dispersion, while the ultimate limit from quantum effects and quantum communication theory has not yet been accurately assessed. To combat the effect of loss for maximizing repeater spacing, optical amplifiers can be used. The recent development of erbium-doped fiber amplifier is a major advance, which operates close to the ideal noise limit of a *phase insensitive linear quantum amplifier* (PIA). For ordinary coherent-state laser sources, an ideal PIA introduces a 3 dB degradation in the signal-to-noise ratio (SNR) for both homodyne and direct detection [1]. With the use of *phase-sensitive linear amplifiers* (PSA), which are parametric amplifiers employed for single-field-quadrature amplification, there is no signal-to-noise degradation at all for homodyne detection [1]. They are also 3 dB better than PIA for direct detection, and is in fact ideal for any source quantum state if phase coherence at the amplifier input is maintained [2]. Such amplifiers in bulk form have been developed at Northwestern University [3], with the goal of adapting them to a fiber-optic environment. The advantage of PSA over PIA is actually much more significant than the 3 dB improvement indicated above. In an amplifier-attenuator chain such as a long-distance fiber-amplifier line, the direct-detection SNR of a PSA system can be a factor of 8 better than that of a PIA line [2]. When the effect of gain saturation is taken into account, many more PSA's can be used in a single line compared to PIA's because in a PSA, the total added quantum noise power is only one fourth that of a PIA [2]. Solitons have been continuing to be developed for combating the effect of dispersion. Very recently, a soliton erbium-amplifier line at 15 Gbits/s and bit error rate $< 10^{-10}$ has been observed over 25,000 km [4]. In such a system, the fiber nonlinearity and *amplifier spontaneous emission* (ASE) noise interact to produce a major limitation on the system. It has been estimated, for example, that a four-fold decrease in ASE noise per unit length could enable a doubling of the system length or repeater spacing [5]. It turns out that the total amplified noise in a PSA amplifier-attenuator chain is also just one-fourth that of a PIA chain [2]. Even more significantly, a PIA soliton line suffers from the Gordon-Haus limitation [6] due to the accumulation of soliton timing error, which is strongly suppressed in a PSA line by a factor of $2G^2$ where $G$ is the amplifier power gain.

Thus, the development and utilization of PSA is clearly a major advance over the erbium-amplifier line. If *photon-number amplifiers* (PNA) are used, there is no degradation for direct detection [1, 7] independently of the nature of the source. However, PNA is presently a device concept without any experimental observation as yet.

These novel quantum amplifiers are also useful in a local network environment. The number of waveguide taps that a passive optical fiber can accommodate is typically quite low, say fewer than 20. One way to increase this number is to employ optical amplifiers. The use of PIA is beset with the problems of ASE and gain saturation [8]. The novel PSA and PNA are again significant in this regard. Furthermore, a waveguide tap has also been proposed on the basis of such amplifiers [9], which is however still limited by noise accumulation and the amount of gain one can employ so that the power in the main bus remains below a threshold level. New device concepts, a *photon-number duplicator* (PND), and similarly a *single-quadrature duplicator* (SQD), have been described via nonlinear optical processes [10]. In particular, they can be used to realize the so-called *quantum nondemolition detection* (QND). The utilization of such duplicators could lead to a *transparent local network* with an indefinitely large number of users, which is impossible with amplifiers [9]-[10].

Dispersion is not a problem for local networks except at ultra-high speeds. However, it is still important to integrate the soliton propagation property with the amplifiers PSA and PNA for long-haul applications. Eventually, soliton duplicators would also be needed for ultra-high speed local networks. All the above discussions presume the use of ordinary coherent-state sources. Finally, intensity and quadrature squeezed sources may be employed to further enhance performance. For squeezed sources only PSA and PNA (or PND and SQD) can be used because PIA destroys the squeezing [1].

The capability of a communication network is also limited by the switching speed. It is therefore important to consider an all-optic mode of operation including both communication and switching. For example, when picosecond pulses are used in 100 Gbits/s system, the switching rate would also have to be in the picosecond range. High speed optical switching is of course also crucial in the realization of fast *all-optical computers.* The problem with the attempt to realize a compact all-optical switch via optical nonlinearity is that very few fast-response materials can achieve a $\pi$ phase shift in less than one absorption length [11]. Optical fiber turns out to be one such material, and all-optical soliton switching with fibers has been experimentally demonstrated [12]. The 0.5 picosecond time-domain switch in that demonstration achieved complete (100%) switching with only 1 pJ of switching energy because of the use of optical solitons to eliminate frequency chirping. However, a very long fiber length $\sim 1$ km is required due to the small fiber nonlinearity, which renders the device impractical and noisy.

# 2 Glossary

| | |
|---|---|
| ASE | amplified spontaneous emission |
| ASK | amplitude shift keying |
| FSK | frequency shift keying |
| GAWBS | guided acoustic-wave Brillouin scattering |
| GVD | group-velocity dispersion |
| LO | local oscillator |
| OOK | on-off keying |
| OPA | optical parametric amplifier |
| PIA | phase-insensitive linear amplifier |
| PNA | photon-number amplifier |
| PND | photon-number duplicator |
| PSA | phase-sensitive linear amplifier |
| PSK | phase shift keying |
| QND | quantum nondemolition detection |
| SNR | signal-to-noise ratio |
| SPM | self-phase modulation |
| SQD | single-quadrature duplicator |
| WDM | wavelength division multiplexing |
| XPM | cross-phase modulation |

# 3 Proposed Goals and Summary of Research Performed

The research program consisted of the following three parts:

**A)** Analysis of Device and System Performance

**B)** Phase-Sensitive Amplification and Duplication of Solitons

**C)** Ultra-Fast All-Optical Switch, Gap Soliton, and Single-Quadrature Duplicator

Below we summarize the proposed goals and the research performed in each of the above areas. A detailed account of the work performed is given in Sec. 4.

## 3.A Analysis of Device and System Performance

The goals of this part of the research were:

1. Theoretically investigate the physical phenomena underlying the quantum devices,
2. Analyse the operation of such devices in a system environment, and
3. Determine the ultimate performance capabilities of optical communication and switching systems within the framework of standard quantum physics.

The following was accomplished:

1. We made a systematic calculation of the noise and timing-error performance of a long-distance fiber link with lumped PSA's for periodic compensation of the in-line loss.
2. We studied various possible realizations of a PNA. A scheme which uses a high-quantum efficiency photodetector followed by a number-state semiconductor laser was found to be promising.
3. We established the ultimate capacity of a power and bandwidth limited lossless optical channel.

## 3.B Phase-Sensitive Amplification and Duplication of Solitons

The goals of this part of the research were:

1. to demonstrate phase-sensitive amplification of solitons and
2. to demonstrate that solitons can be duplicated.

Below we summarize the research performed towards achieving the above goals. Along the way we also discovered some new properties of PSA's, such as their ability to compensate dispersion and their use in soliton storage rings.

### 3.B.1 Phase-Sensitive Amplification of Solitons

- We sytematically analyzed, first classically and then quantum mechanically, the evolution of soliton-like pulses in a nonlinear fiber line in which linear loss is balanced by a chain of periodically-spaced PSA's.

- We proposed a novel approach to combating the pulse broadening effect of group-velocity dispersion (GVD) in a fiber-optic communication link. Our approach relies on the use of PSA's to amplify and shape the short pulses propagating in the fiber. Since our scheme does not rely on the formation of solitons in the fiber, it can be implemented in both the positive as well as the negative GVD regions of the fiber, and it does not require a minimum peak power for the short pulses. Experiments to demonstrate the dispersion compensation property of PSA's could not be finished due to excessive phase noise on our laser. Work is underway to phase stabilize the laser.

- We demonstrated the implementation of an all-fiber PSA at $\lambda = 1.5\,\mu$m using the nonlinear index $n_2$ of fused-silica fiber. A picosecond saturable-absorber mode-locked Er/Yb fiber laser was used as the source of solitons.

- We proposed long-term storage of a soliton bit stream in a fiber ring in which loss is compensated by phase-sensitive amplification. We showed that the one's (soliton pulses) are asymptotically stable and the noise on the zero's of the bit stream (absence of a soliton) is bounded. Such storage devices will be useful as interchange and routing buffers and will be compatible with wavelength division multiplexed (WDM) all-optical soliton networks. Memory elements can be designed that will hold over 10 Mbits of data for almost an indefinite period of time with access time as short as $1\,\mu$s.

### 3.B.2 Photon Duplication of Solitons

We could not demonstrate photon duplication of solitons because of excessive scattering from the CdTe samples used in the experiments. Work is currently underway to use other semiconductor materials and to understand the physical nature of the scattering process.

## 3.C Ultra-Fast All-Optical Switch, Gap Soliton, and Single-Quadrature Duplicator

The goals of this part of the program were:

1. to demonstrate semiconductor based compact ultrafast all-optical switch that approaches the practicality criterion,

2. to demonstrate improved switching using either birefringence or gap soliton propagation [13], and

3. to demonstrate a semiconductor $n^{(2)}$ based optical parametric amplifier using either AlGaAs or InGaP waveguide and to show that it is quantum-limited, and then to demonstrate single-quadrature duplication with it.

### 3.C.1 Compact Ultrafast All-Optical Switch

- We successfully fabricated 1 cm long, low loss strongly-guided AlGaAs waveguides with 1.5$\mu$m by 1.5$\mu$m physical cross sectional area and 0.8$\mu$m by 0.9$\mu$m fundamental mode cross sectional area.

- We successfully demonstrated ultrafast all-optical switching using AlGaAs waveguide operating at 1.6$\mu$m. For a 1cm long microfabricated strongly guiding waveguide with 0.8$\mu$m by 0.9$\mu$m fundamental mode cross sectional area, switching is achieved with an average power of 1.2mW for 82 MHz mode-locked 430 fsec pulses. The estimated peak power and pulse energy inside the microfabricated waveguide were $\sim$30 W and $\sim$14.6 pJ, respectively, which is 5–10 times lower than the values needed with conventional waveguides. For a conventional 9mm long rib waveguide with 4.5$\mu$m by 2.7$\mu$m mode cross sectional area, switching is achieved at a much higher peak power of 550 W.

- We successfully developed and demonstrated a new experimental technique that allows the simultaneous measurement of the nonlinear refractive index $n^{(2)}$ and the nonlinear absorption coefficient $\alpha^{(2)}$ in waveguides. By performing minor changes in the experimental setup, the four-wave mixing gain coefficient can also be measured.

### 3.C.2 Improved Ultrafast All-Optical Switch with Gap Soliton Propagation

- We successfully fabricated very broadband Bragg reflectors in microfabricated AlGaAs optical waveguides with bandwidths as large as 5-10 nm. They could be used as wavelength selective filters for short 100fsecs pulses in waveguides or for gap soliton propagation.

- We successfully investigated theoretically the propagation of coupled Bragg solitons for all-optical switching.

- The experimental investigation of Bragg solitons has not been successful within the term of the contract due to the needs for higher laser power to form gap solitons. Ultimately, the formation of gap solitons may be limited by multi-photon absorption.

### 3.C.3 Single-Quadrature Duplicator

- We successfully investigated theoretically the generation of squeezed-state light in AlGaAs semiconductor waveguides.

- We successfully demonstrated degenerate optical parametric amplification in AlGaAs semiconductor waveguides at 1.6$\mu$m using a new single-pass pulsed delayed scheme to filter out the pump intensity. A power gain of more than 8 was observed. This demonstration shows the possibility of using the scheme for squeezed-state generation via parametric deamplification of quantum noise, which is needed for single-quadrature duplication. The degenerate optical parametric amplification demonstrated is however potentially useful in optical communications.

- We successfully demonstrated frequency translation in AlGaAs semiconductor waveguides at 1.6$\mu$m using a single-pass scheme. The setup used was a slight variation of the parametric amplifier setup. A four-wave-mixing gain of larger than unity was observed. Frequency translation is potentially useful in optical communications.

- The experiment to generate squeezed state was not completed within the contract period due to excess classical noise in our laser, which masked the quantum noise reduction.

# 4 Details of Research Performed and Outcomes

The research program comprised of three main parts, each directed by one of the three co-principal investigators. Below we describe in detail the research performed under this contract. A separate section is devoted to each of the three main parts.

## 4.A Analysis of Device and System Performance

The goals of this part of the research program directed by Yuen were:

1. to theoretically investigate the physical phenomena underlying the quantum devices,
2. to analyse the operation of such devices in a system environment, and
3. to determine within the framework of standard quantum physics the ultimate performance capabilities of optical communication and switching systems.

Below we describe the research performed on each of the proposed items.

### 4.A.1 Performance of Systems that Utilize Novel Quantum Devices

We have made a systematic calculation of the noise and timing-error performance of a long-distance fiber link with lumped phase-sensitive linear amplifiers (PSA) for periodic compensation of the in-line loss. Let $\Gamma$ be the loss coefficient per unit length, $L$ the total length of the link, $S$ the transmitted signal photon level, $G$ the power gain of each of the identical PSA's, and $A$ and $N_0$ characteristics of the signal pulse amplitude and energy. The output direct-detection signal-to-noise ratio and timing-error variance for a PSA chain are found to be

$$\left(\frac{S}{N}\right)_{PSA} \sim \frac{\ln G}{G-1}\frac{S}{\Gamma L}, \tag{1}$$

$$\langle \delta t^2 \rangle_{PSA} \sim \frac{A}{6N_0}\frac{L}{2\Gamma}\frac{\ln G}{G-1}. \tag{2}$$

These can be compared to the standard results in the ordinary phase-insensitive linear amplifier (PIA) chain:

$$\left(\frac{S}{N}\right)_{PIA} \sim \frac{\ln G}{G-1}\frac{S}{2\Gamma L}, \tag{3}$$

$$\langle \delta t^2 \rangle_{PIA} \sim \frac{2A\Gamma}{9N_0}L^3\frac{G-1}{\ln G}. \tag{4}$$

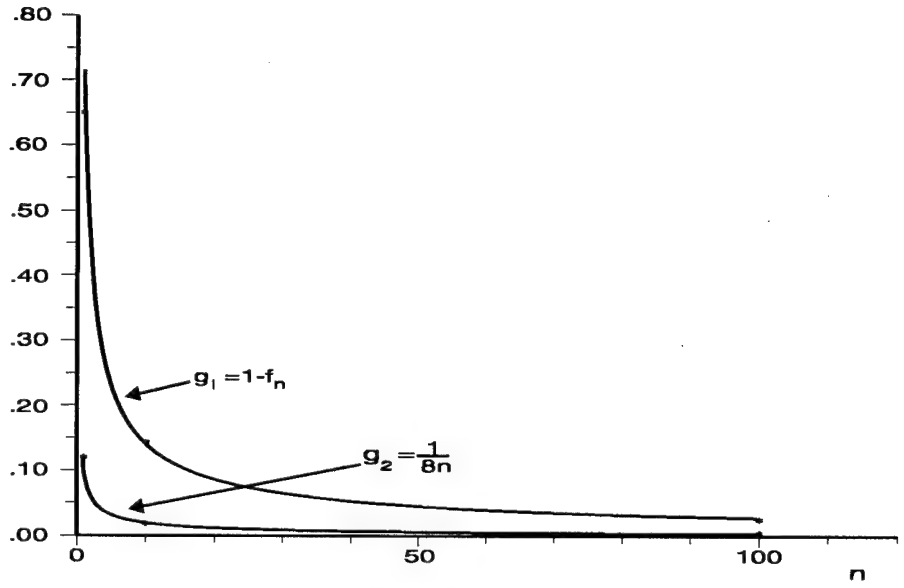


Figure 1: Error exponents per signal photon as a function of number of amplifier stages with gain G=10; $g_1$ applies to a PNA line and $g_2$ to a PIA line under the Gaussian approximation.

From Eqs. (1)–(4) the signal-to-noise ratio for the PSA chain is enhanced by a factor of two while the timing error is suppressed by a factor of $E^{-1}$ compared to a PIA chain,

$$E^{-1} = \frac{3}{8(\Gamma L)^2}\left(\frac{\ln G}{G-1}\right)^2. \tag{5}$$

For typical values $L \sim 10^4$ km, $2\Gamma \sim 0.055$ km$^{-1}$ (for 0.24 dB/km), $G \sim 10$ dB, the timing-error $\Delta t \equiv \sqrt{\langle \delta t^2 \rangle}$ is decreased by three orders of magnitude from Eq. (5). In terms of bit rate $R$ increase for the two kinds of chains, this translates into about a factor of seventy for typical soliton pulses in binary signaling.

We have obtained the following result for the OOK error probability $P_e$ of a PNA line of gain $G$ for each amplifier. For $n$ stages of amplification-attenuation of coherent-state input with signal photon number $n_s$,

$$P_e = \frac{1}{2}e^{-n_s(1-f_n(G))}, \tag{6}$$

where the function $f_n$ obeys the recurrence relation

$$f_{n+1}(G) = \left(1-G^{-1}\right)^G \left[1 + f_n(G)(G-1)/G\right]^G, \tag{7}$$

with $f_0(G) = 0$. In Fig. 1 we compare this error exponent $1 - f_n(G)$ with that of the PIA chain $1/8n$ obtained under the Gaussian approximation. The advantage of the PNA line increases from a factor of $\sim 5$ for a single stage to a factor of $\sim 20$ for $n \geq 50$ stages. The

actual error exponent of a PIA chain has never been exactly determined, which may turn out to be somewhat better than that of the Gaussian approximation. However, the advantage of a PNA over PIA or even PSA goes far beyond the ideal-system error exponent. Because *no* (or little, in a good but realistic implementation) noise is added to the communication line, the flexibility of system design and implementation is greatly increased. For example, nonlinear phase distortion in the line would be minimal. Similarly, we expect that PNA action would not disturb soliton propagation in a long line.

### 4.A.1 Physics of the Novel Quantum Devices

We studied various possible realizations of a PNA. A scheme which uses a high-quantum efficiency photodetector followed by a number-state semiconductor laser [14] was found to be promising. We concluded that this realization of the PNA is not significantly limited by the electronic amplifier noise or the laser quantum efficiency for input states that are nearly classical.

### 4.A.2 Ultimate Quantum Limit Performance Study

We established the ultimate capacity of a power and bandwidth limited lossless optical channel [15]. The possible amount of information transfer between any source and any user via a quantum system is bounded through the quantum entropy function. In contrast to the classical case, this shows that an infinite information transfer implies infinite emtropy. The entropy bound was applied to obtain the ultimate quantum information transmission capacity of the free electromagnetic field unmder a power and bandwidth constraint. Extension of our results to a lossy system is still under investigation.

## 4.B Phase-Sensitive Amplification and Duplication of Solitons

The goals of the experimental research undertaken by Kumar were:

1. to demonstrate phase-sensitive amplification of solitons and
2. to demonstrate that solitons can be duplicated.

Below we describe the research performed towards achieving the above goals. Along the way we also discovered some new properties of PSA's, such as their ability to compensate dispersion and their use in soliton storage rings. Details of these discoveries are also given in the following.

### 4.B.1 Phase-Sensitive Amplification of Solitons

We investigated both the theoretical as well as experimental aspects of using PSA's in ultra-high speed communication systems and networks.

Yuen [2] was the first to point out the advantages of using PSA's in optical communication systems (long haul or local network) that employ solitons as the carriers of information. Solitons are pulses of light that balance the linear group-velocity dispersion of a single-mode fiber with the Kerr-nonlinearity generated self-phase modulation. As a result of the balance, solitons can propagate over long distances without changing their shape. The advantages of such pulses as carriers of information are obvious as they avoid cross-talk between successive bits [5, 16]. In both long haul and local network systems, however, solitons must be periodically amplified to compensate for the linear propagation loss. Recently erbium-doped fiber amplifiers have been developed that operate very close to the ideal quantum-mechanical limit. These amplifiers degrade the solitons upon repeated amplification, as would be required in a realistic system, because of the added spontaneous emission noise. Yuen's analysis showed that if a PSA of gain $G$ is used in place of a PIA (e.g., the erbium amplifier) of the same gain, then the following advantages could be realized [2]:

i) The PSA reduces the total added quantum noise power by a factor of 4.

ii) The PSA reduces the homodyne noise variance by a factor of 2.

iii) The PSA reduces the photon-number variance by a factor of between 2 to 8 depending upon the number of inline amplifiers.

iv) The PSA suppresses the Kerr-effect phase fluctuation variance by a factor of $2G^2$.

v) The PSA suppresses the Gordon-Haus soliton timing error by a factor of $2G^2$.

The above predictions of Yuen, however, were based on a single-mode quantum analysis of the fiber/PSA line. Soliton evolution from one amplifier to the next was ignored. As part of this contract we have sytematically analyzed, first classically [17, 18] and then quantum mechanically [19], the evolution of soliton-like pulses in a nonlinear fiber line in which linear loss is balanced by a chain of periodically-spaced PSA's, as sketched in Fig. 2

### 4.B.2 Solitons in fiber lines with PSA's

The use of lumped erbium-doped fiber amplifiers has been demonstrated as an effective method for compensating loss in long-distance optical communications systems [20, 21, 22]. In addition, several filtering techniques [23] have been developed for soliton-based systems

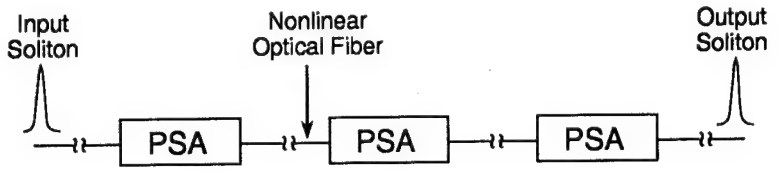


Figure 2: Schematic of a nonlinear optical fiber transmission line in which loss is balanced by a chain of periodically-spaced, phase-sensitive amplifiers (PSA's).

which decrease the Gordon-Haus jitter [5] — the random walk of solitons caused by spontaneous emission noise present in the erbium-doped amplifiers, or by acoustic perturbations [24] — thereby increasing the maximum allowable bit rate.

As a possible alternative to erbium-doped fiber amplifiers, the use of lumped PSA's has been proposed [25] as a method for compensating loss. Because phase-sensitive amplifiers are free of spontaneous emission noise [25] (they are ideal quantum-limited amplifiers with a 0 dB noise figure), they add no Gordon-Haus jitter to the propagating solitons and therefore lead to a significant increase in the maximum bit rate [26]. A PSA can also be thought of as a combination of an amplifier and a filter integrated into one device. In this sense, they are analogous to the erbium amplifiers and passive filters used in the schemes mentioned above. For PSA's, however, the filtering is done in the signal's optical phase, rather than only in the frequency domain, since only one phase quadrature is amplified while the other quadrature is attenuated (or filtered out) by the PSA's.

In our analyses [17, 18] we considered the practically-encountered case in which the amplifier spacing is much smaller than the dispersion length, i.e., the loss experienced by the pulse due to the fiber and the gain associated with the PSA occur on a length scale much shorter than that of the dispersion and nonlinearity. In our approach, we averaged over the rapid fluctuations due to the loss and gain [21] and analyzed the averaged equation governing the pulse evolution over distances much greater than the dispersion length. The averaged envelope equation supports stable pulse propagation, and initial pulses were shown to decay exponentially onto steady state solutions. This is in contrast with the case of a fiber line with erbium amplifiers for which pulse stability is reached via the shedding of dispersive radiation [21, 22].

Our analysis also showed that the length scale over which the pulse evolution occurs is significantly increased beyond a soliton period. This is because of the attenuation of phase variations across the pulse's profile by the amplifiers. Analytical evidence was presented which indicated that stable pulse evolution occurs on length scales much longer than the soliton period. This was confirmed through extensive numerical simulation, and the region of stable pulse propagation was found. The average evolution of such pulses is governed by a

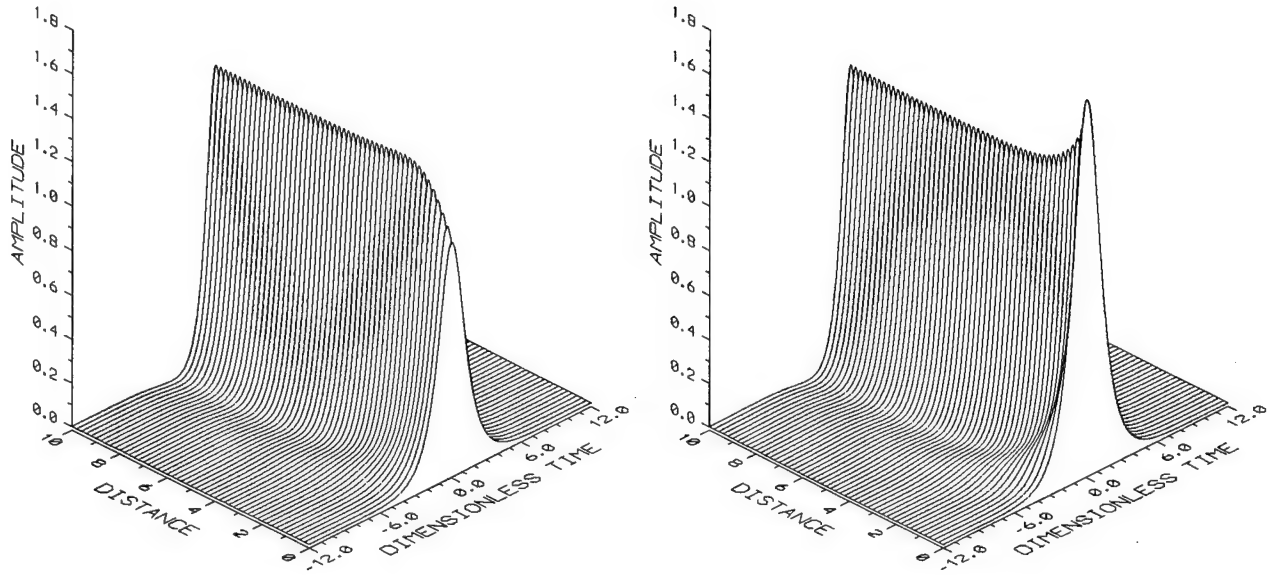


Figure 3: Evolution of initial pulses $U(T,0) = \operatorname{sech} T$, (left), and $U(T,0) = 1.8 \operatorname{sech} T$, (right), showing exponential decay onto the stable pulse solution of the fiber-PSA line.

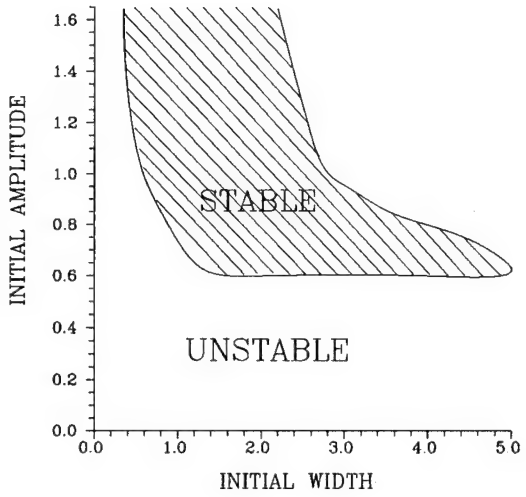


Figure 4: Initial pulse amplitudes $A$ and widths $T_0$ which give stable pulse solutions. The initial conditions $U(T,0) = A \operatorname{sech}(T/T_0)$, with different values of $A$ and $T_0$, were used. For all initial conditions within the lined region the same final steady-state was reached.

fourth-order nonlinear diffusion equation which describes the exponential decay of arbitrary initial pulses onto stable, steady-state, soliton-like pulses.

Figure 3 shows two representative numerical simulations of pulse propagation. Figure 3a is for an initial pulse $U(T,0) = \operatorname{sech} T$ and Fig. 3b for $U(T,0) = 1.8 \operatorname{sech} T$. In both cases the pulse exponentially approaches a stable steady state as it evolves. The parameters used in this computation correspond to an amplifier spacing and gain of roughly 36 km and 2.72, respectively. The pulses in these simulations propagate 10 units in the dimensionless units, which corresponds physically to a pulse traveling through 2,750 amplifiers for a total distance of roughly 105,696 km. Such a long distance was chosen to explicitly show the stability of the pulses.

Figure 4 shows that a wide range of initial pulse amplitudes and widths can lead to stable pulse evolution. This data was obtained by simulating the propagation for many different initial pulses of the form $U(T,0) = A \operatorname{sech}(T/T_0)$ with different values of $A$ and $T_0$ and recording the cases in which the stable steady-state pulse solution was reached. Note that all initial pulses within the shaded region asymptote to the same stable steady state. The numerical simulations were done using the same parameter values as in Fig. 3, Similar numerical runs indicate that stable pulse solutions are also obtained for a wide range of amplifier spacings, such as 72 km. Further details of the analysis and numerical simulations can be found in Ref. [18].

Our analysis also provides a physical explanation for the above results. Upon propagation through a segment of the fiber, the pulse is attenuated by the loss and develops a quadratic phase sweep across its profile since group-velocity dispersion and self-phase modulation do not exactly balance one another as the pulse decays. The phase-sensitive amplifiers, however, work to produce an output pulse that is uniform in phase; the phase sweep induced in the pulse is therefore attenuated by the PSA's, canceling the effects of the dispersion and self-phase modulation. Thus, the PSA's act as phase-sensitive filters (analogously to lock-in amplifiers) that fight dispersion and other pulse-deforming effects. The argument also implies that the cancellation effect does not necessarily depend on self-phase modulation being present. As a result, phase-sensitive amplifiers can be used to compensate dispersion in fiber optic communication systems where the nonlinearity of the fiber plays no role. As part of this contract, we have studied the dispersion compensation property of PSA's in great detail [27, 28]. In the following, we provide a summary of this work.

### 4.B.3 Dispersion compensation with PSA's

An important limitation to the bit-rate distance product achievable in a fiber-optic communication link arises because of the group-velocity dispersion (GVD) in the fiber [29, 30]. At

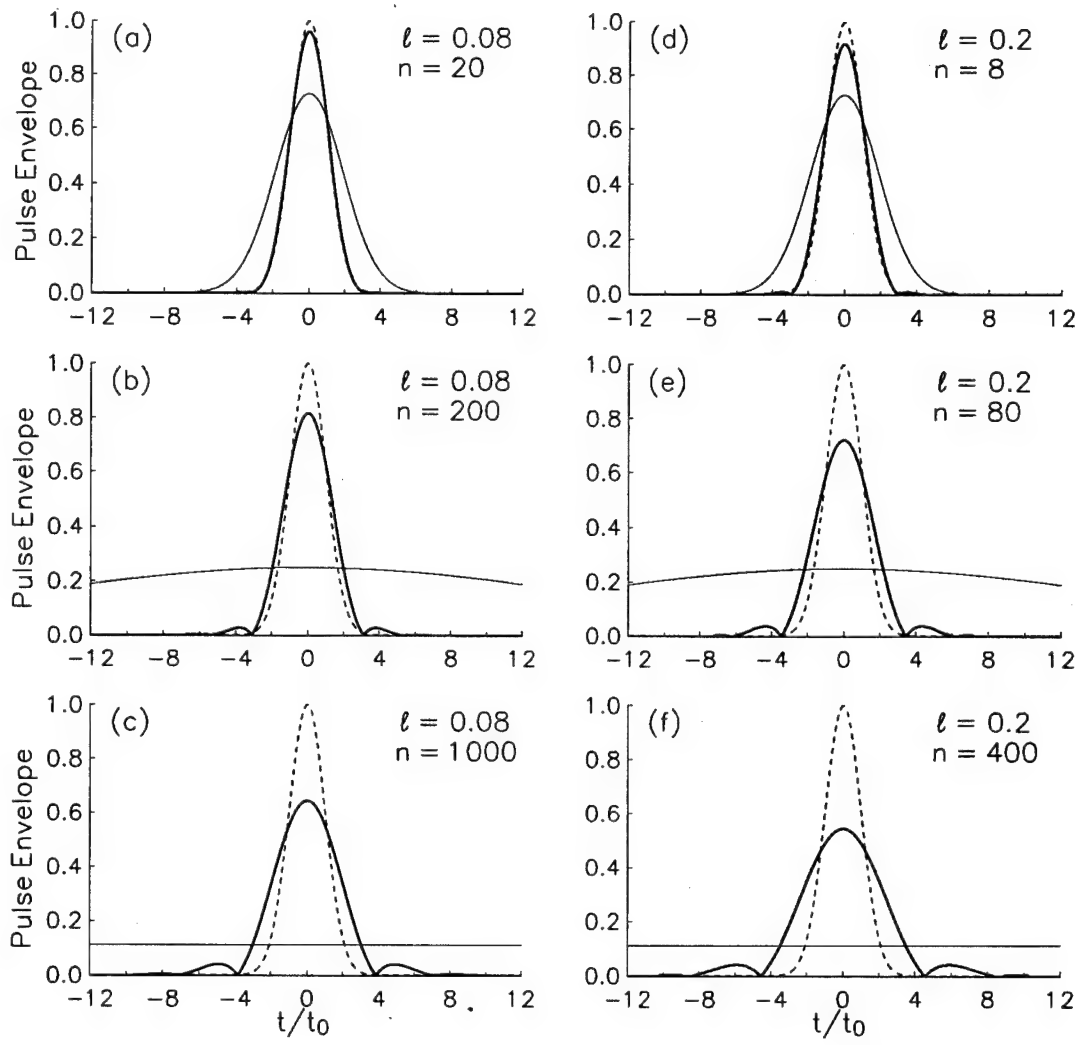


Figure 5: Magnitude of a Gaussian input pulse (dashed curves) propagating through the fiber/PSA line with $\ell = 0.08$ [plots (a) through (c)] and $\ell = 0.2$ [plots (d) through (f)]. Here $\ell$ is the ratio of the amplifier spacing to the dispersion length. In each plot the thick solid curve shows the pulse at the output of the $n$th amplifier with $n$ as indicated in the plots and the thin solid curve shows the pulse that would result if phase-insensitive amplifiers (such as EDFA's for the 1.55 $\mu$m link) are used. In plots (a) through (c) the amplifier spacing is 2.4 km and in plots (d) through (f) it is 40 km.

higher bit rates, the dispersion-induced broadening of short pulses propagating in the fiber causes cross-talk between the adjacent time slots, leading to errors when the communication distance increases beyond the dispersion length $z_c$ of the fiber. Here $z_c = t_0^2/|k''|$, where $t_0$ is the width of the short pulses, $k'' = \partial^2 k/\partial\omega^2$ evaluated at the carrier frequency $\omega_0$, and $k$ is the propagation constant in the fiber.

Several approaches have been followed to push the bit-rate–distance product to higher values. One approach is to use solitons as the information bits [31]. Solitons, which are nonlinear pulses that preserve their shape upon propagation through the fiber, are formed when the carrier frequency lies in the negative GVD region of the fiber—i.e., $k'' < 0$. In this region the positive Kerr nonlinearity of the fiber works to cancel the broadening caused by the negative GVD. However, in fused silica fibers, the negative GVD region occurs for wavelengths longer than $1.3\,\mu$m. In this wavelength region, convenient semiconductor short-pulse lasers are still not widely available for use as soliton sources, especially when one pushes the bit rates to increasingly higher values which would require shorter pulses with correspondingly higher peak powers to form solitons [32].

Many other approaches that have recently been proposed and demonstrated include the use of various forms of inline optical filters [33, 34], prechirping of the transmitting laser [35], use of inline equalizing fiber [36], and nondegenerate four-wave mixing [37, 38]. The most successful among these various techniques uses periodically-spaced segments of a two-mode fiber operated near cut-off [39] that provide positive (negative) GVD to the propagating pulse to compensate the negative (positive) GVD that occurs in the single-mode fiber spans. This technique, however, requires the use of spatial mode converters between the single-mode and the two-mode fiber segments.

We have proposed a novel approach to combating the pulse broadening effect of GVD in a fiber-optic communication link [27]. Our approach relies on the use of phase-dependent amplifiers to amplify and shape the short pulses propagating in the fiber. Moreover, our scheme does not rely on the formation of solitons in the fiber. Therefore, it can be implemented in both the positive as well as the negative GVD regions, and it does not require a minimum peak power for the short pulses.

In our scheme linear loss in the fiber is balanced by a chain of periodically-spaced, phase-sensitive, optical amplifiers. We presented detailed analysis of pulse propagation in such a fiber line showing that due to attenuation in the quadrature orthogonal to the amplified quadrature it is possible for a pulse to propagate without significant broadening over lengths many times longer than the usual dispersion length of the fiber [28].

To demonstrate that the spreading of the pulse is curtailed with use of the PSA's, we numerically simulated with our theory the propagation of short Gaussian pulses in a fiber/PSA

line. As a first example, we considered a communication link that operates at 0.8 $\mu$m wavelength. At this wavelength, the loss and GVD coefficients of a typical fused silica fiber are 2.0 dB/km and 30 ps$^2$/km, respectively. If 30 ps pulses are used, then the dispersion length of such a fiber is 30 km [30]. Placing PSA's of 4.8 dB gain every 2.4 km will result in a lossless fiber line. In Fig. 5, plots (a) through (c), we show the amplitude of the propagating pulse at different locations in such a fiber/PSA line. Also shown in each case are the amplitudes of the original Gaussian pulse (dashed curves) and the pulse that would result if phase-insensitive amplifiers are used (thin solid curves). As is evident in Fig. 5c, at the output of the 1,000th amplifier—a distance of 2,400 km in this case (80 dispersion lengths)—the pulse shape, apart from developing small oscillations in the wings, is pretty much unchanged. For the case of phase-insensitive amplifiers, on the other hand, the pulse is completely flattened out.

Our second example was a communication link operating at 1.55 $\mu$m wavelength. At this wavelength, the loss and GVD coefficients of a typical dispersion-shifted fused silica fiber are 0.2 dB/km and $-2$ ps$^2$/km, respectively [30]. If 20 ps pulses are used, then the dispersion length of such a fiber is 200 km. Placing PSA's of 8 dB gain every 40 km will result in a lossless fiber line. In Fig. 5, plots (d) through (f), we show the amplitude of the propagating pulse at different locations in this fiber/PSA line. Once again, at the output of the 400th amplifier—a distance of 16,000 km in this case (80 dispersion lengths)—the pulse shape, apart from developing small oscillations in the wings, is pretty much unchanged.

We also derived an averaged equation for pulse evolution over distances longer than the amplifier spacing. The effect of optical-phase fluctuations between the propagating pulse and the amplifiers was also considered. Further details can be found in Ref. [28].

We carried out an experiment to demonstrate the dispersion compensation property of the PSA's. This experiment, however, was not successful because of the excessive phase noise on our laser. As described in the following section, large PSA gain could be observed when both the signal and pump pulses were derived from the same laser pulse. To demonstrate dispersion compensation, however, the signal pulse must be repetitively amplified with successive pump pulses. In our experiment, no PSA gain could be observed when the pump pulse was derived from a laser pulse that is 25 pulses down stream from the signal pulse. This lack of observation of the PSA gain is a direct manifestation of the phase noise on our laser. Work is currently underway to phase stabilize our laser so that we could repeat the dispersion compensation experiment.

### 4.B.4 Fiber PSA's

As part of this contract we have also demonstrated the implementation of an all-fiber PSA at $\lambda = 1.5\,\mu$m using the nonlinear index $n_2$ of fused-silica fiber. This work was performed

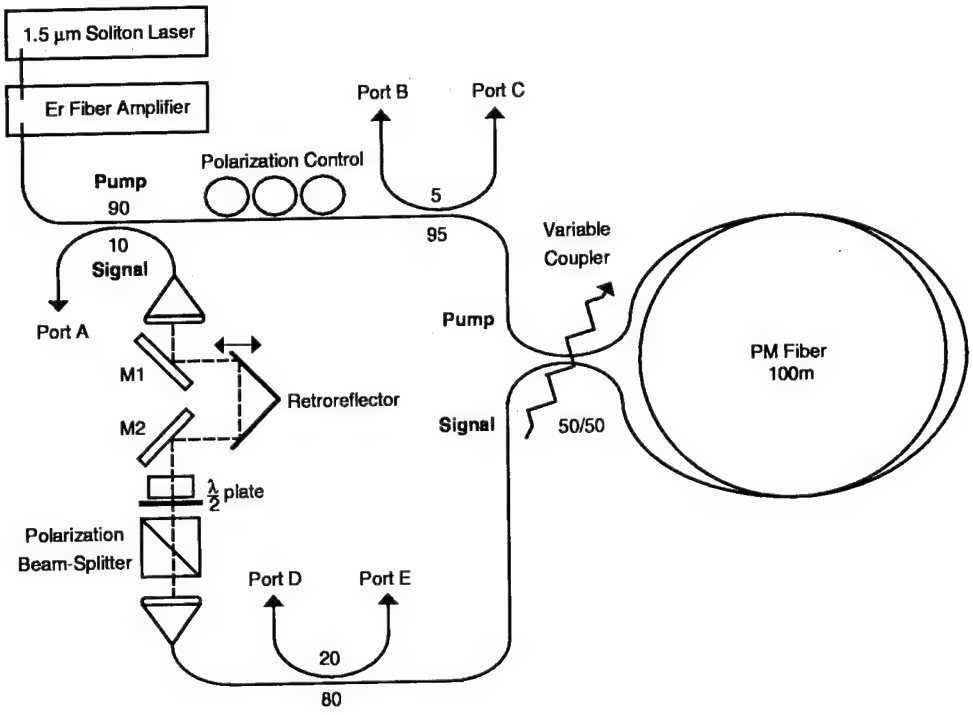


Figure 6: Schematic diagram of the 1.5 $\mu$m picosecond-pulse fiber PSA.

in collaboration with Dr. K. V. Reddy of Amoco Technology Company. 8.3 ps pulses were amplified in a phase-sensitive way using a Sagnac interferometer as shown in Fig. 6. For non-zero input signal power $I_s$ and pump power $I_p$ the gain of such an amplifier is found to be [40]

$$\begin{aligned} G &= \cos^2(\Delta\Phi_{NL}) + (I_p/I_s)\sin^2(\Delta\Phi_{NL}) \\ &\quad - (I_p/I_s)^{1/2}\sin(2\Delta\Phi_{NL})\sin\delta, \end{aligned} \tag{8}$$

where $\Delta\Phi_{NL} = \kappa L(I_p I_s)^{1/2}\cos\delta$, $\kappa = 2\pi n_2/\lambda A_{\text{eff}}$ with $A_{\text{eff}}$ as the effective fiber-core area, $L$ is the length of the fiber, and $\delta$ is the phase difference between the pump and signal fields. For fused-silica fiber $n_2 = 3.2 \times 10^{-20}\,\text{m}^2/\text{W}$.

In the experiment of Fig. 6 we used 100 m of polarization-preserving fiber in the Sagnac interferometer. The laser source was a 1.5 $\mu$m mode-locked Er-fiber laser with a pulse width of 8.3 ps at a pulse repetition rate of 23.4 MHz, amplified by a fiber amplifier to generate an average power up to 11.0 mW in the pump arm. We used a series of polarization controllers to maximize the pump light along one axis of the fiber. Also a translating retroreflector was used in the signal arm for pump/signal pulse synchronization. The signal beam was launched into the Sagnac loop with the same polarization as the pump so that phase-sensitive self-phase modulation due to the superposition of the pump and signal pulses would occur, which is our gain mechanism. We used a variable fiber coupler in the Sagnac interferometer

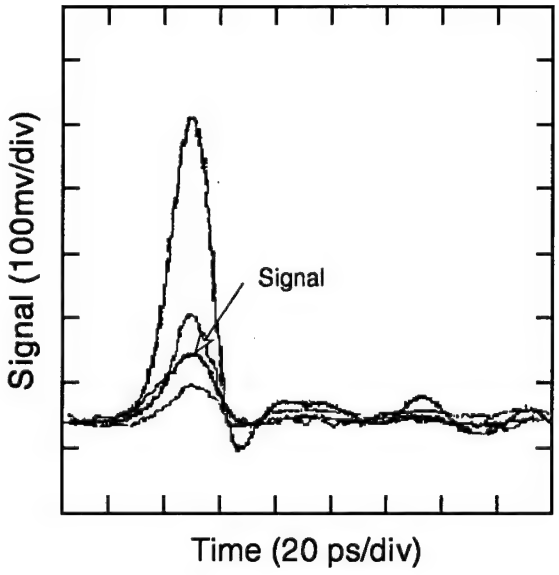


Figure 7: Phase dependence of the signal amplification for $I_s$=40 $\mu$W and $I_p$=2 mW.

to ensure exact 50/50 coupling along the two directions, and thus, maintained good isolation of the pump beam from the signal arm.

After the signal and pump pulses were aligned, we observed the reflected signal light at port D for average input signal powers up to 300 $\mu$W. Without phase locking, the amplified signal pulse modulated from a deamplified minimum to a highly amplified maximum due to fluctuations in the path lengths of the signal and pump pulses from the laser to the Sagnac interferometer, as shown in Fig. 7. The observed amplification and deamplification of the reflected signal was consistent with the theory presented in Eq. (8). Figure 8 shows one set of experimental data taken at port D, with pump leakage into the signal arm (indistinguishable from the background noise), the signal pulse, and the amplified pulse resulting from the interaction of the pump and signal. Here the average pump and signal powers were 3.0 mW and 40 $\mu$W, respectively. The amplified signal pulse is 6.5 times larger than the input signal pulse, for a gain of 8.2 dB. We have observed gains as high as 10 dB.

This gain is clearly the result of amplification of the signal as it is much higher than what would be expected from interference of the reflected signal and the leakage pump in the signal arm. We observed that the gain for different signal powers (much smaller than the pump) with the same pump power given above remained constant. This is consistent with our expectations from Eq. (8) since the pump power is much greater than the signal power; hence amplification is dependent only on the pump power. In Fig. 9 we show the dependence of the gain on the pump power. The measured gain (squares) is consistent with the predictions of Eq. (8) (solid curve) based on self-phase modulation in the Sagnac interferometer. An increase in the pump power will lead to an increase in the gain and we

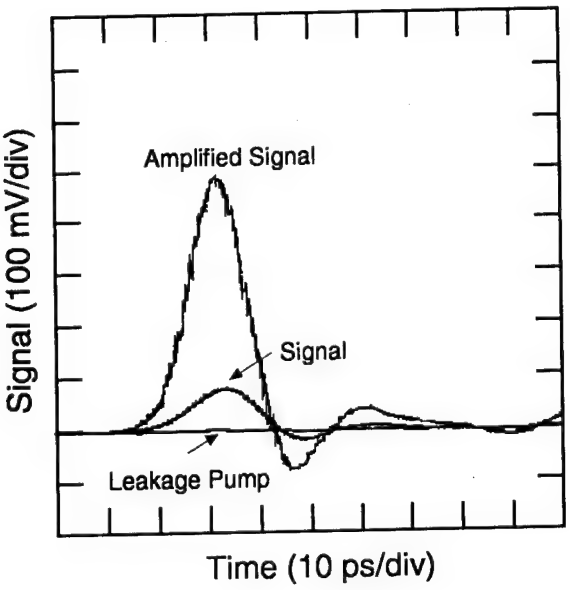


Figure 8: Phase-sensitive amplification of 8.3 ps pulses at 1.5 $\mu$m. The signals were monitored using a 45 GHz photodiode and a 50 GHz sampling oscilloscope.

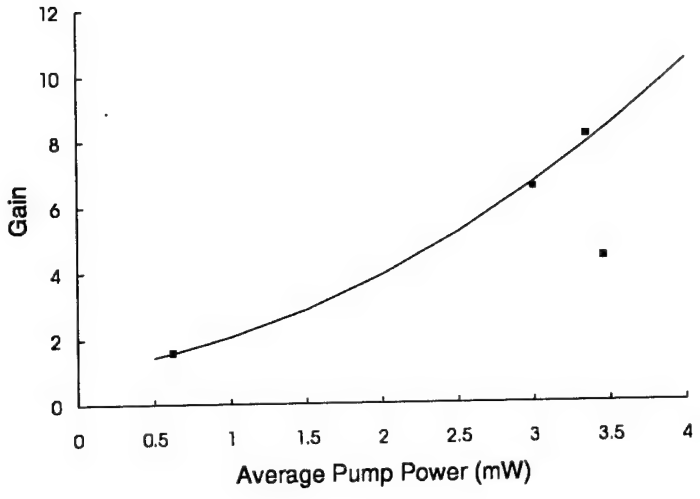


Figure 9: Maximum gain as a function of the average pump power. The squares are the data points whereas the solid curve shows the theoretically expected gain.

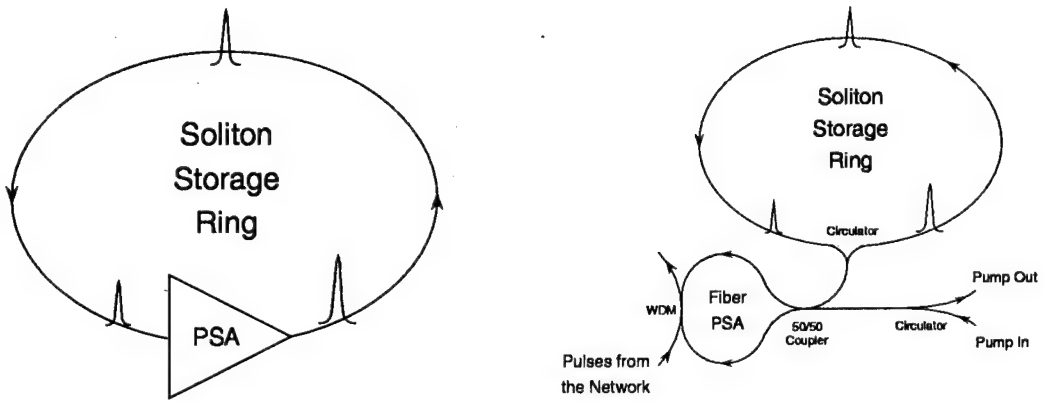


Figure 10: Left – Schematic of a fiber ring in which loss is compensated by phase-sensitive amplification. Right – A physically realizable optical storage ring using a fiber PSA [41]. Note that the storage ring can be loaded without keeping track of the optical phase of the data stream on the network.

expect to observe up to 30 dB of gain.

Our observations lead us to believe that a 1.5 $\mu$m fiber/PSA line can be implemented with high gain, low noise, and negligible dispersion.

### 4.B.5 Storage of soliton bit streams using PSA's

We proposed long-term storage of a soliton bit stream in a fiber ring in which loss is compensated by phase-sensitive amplification [19]. We showed that the one's (soliton pulses) are asymptotically stable and the noise on the zero's of the bit stream (absence of a soliton) is bounded. Moreover, the soliton-soliton interaction is efficiently suppressed by the PSA's.

Such storage devices will be useful as interchange and routing buffers and will be compatible with wavelength division multiplexed (WDM) all-optical soliton networks. Memory elements can be designed that will hold over 10 Mbits of data for almost an indefinite period of time with access time as short as 1 $\mu$s.

Consider an optical fiber ring with a PSA as shown in Fig. 10(Left). Since the PSA is a unidirectional device, pulses traveling only in one direction (counter-clockwise in the case shown) around the loop see the linear loss compensated by the amplifier. A 3 km-long loop made out of a dispersion-shifted fiber having $|\beta''| = 0.2\,\mathrm{ps}^2/\mathrm{km}$ and $\gamma = 0.017\,\mathrm{km}^{-1}$ (0.15 dB power loss per km) would serve the purpose. If such a ring is used to store streams of bits with a period of 10 ps [bit rate of 100 Gbits/s with 1's represented by 3.5 ps (FWHM) pulses and 0's by the absence of pulses], then the dispersion and loss lengths would be $z_0 \equiv \tau^2/|\beta''| = 20\,\mathrm{km}$ and $z_\gamma \equiv 1/2\gamma = 29.4\,\mathrm{km}$, respectively. For these parameters, our analysis and numerical simulations showed that the data could be stored indefinitely in such a ring [19]. The ring would have a storage capacity of 1.5 Mbits and it can be built using a

fiber PSA [41] as shown schematically in Fig. 10(Right). Figure 10(Right) also shows how the storage ring can be loaded without keeping track of the optical phase of the data stream on the network. The 1's of the incoming data stream imbalance the Sagnac loop of the PSA through cross-phase modulation. Consequently, a pulse is injected into the storage loop that is phase coherent with the pump laser driving the PSA. The incoming 0's, however, do not cause cross-phase modulation, and hence, no pulse is injected into the storage loop. Since there is no phase coherence between the network and the storage ring, such a device is thus intrinsically WDM compatible.

### 4.B.6 Photon Duplication of Solitons

We could not demonstrate photon duplication of solitons because of excessive scattering from the CdTe samples. At high pump intensities where photon duplication is expected to occur, linear scattering of the pump photons in the direction of the signal and conjugate beams prevented the observation of the duplication phenomenon. These results were presented at the 1994 OSA annual meeting in Dallas. Work is currently underway to use other semiconductor materials and to understand the physical nature of the scattering process.

## 4.C Ultra-Fast All-Optical Switch, Gap Soliton, and Single-Quadrature Duplicator

The basic program of research proposed by Ho consisted of work:

1. to demonstrate semiconductor based compact ultrafast all-optical switch that approaches the practicality criterion,
2. to demonstrate improved switching using either birefringence or gap soliton propagation, and
3. to demonstrate a semiconductor $n^{(2)}$ based optical parametric amplifier using either AlGaAs or InGaP waveguide and to show that it is quantum-limited, and then to demonstrate single-quadrature duplication with it.

### 4.C.1 Compact Ultrafast All-Optical Switch

As mentioned in the introduction, the capability of a communication network—be it a local network or long haul fiber network—is limited by the switching speed. All-optical switching has been demonstrated in various configurations such as the nonlinear directional coupler [42] and the asymmetric Mach-Zehnder interferometer [43]. However, for an optical switch to be practical, it is necessary for the device to be operated at low peak power and also be compact

in size, which requires nonlinear materials with high nonlinearity and low loss. A measure of a material's usefulness for optical switching applications is given by a figure of merit [42, 44] defined as $F = n^{(2)}\mathrm{I}/(\alpha\lambda)$, where $n^{(2)}$ is the second order nonlinear refractive index, $\alpha$ is the total (linear and nonlinear) absorption coefficient, I is the laser intensity needed to achieve optical switching (determined by $n^{(2)}$ and the medium's length), and $\lambda$ is the free space optical wavelength. In order for a material to be usable for all-optical switching, it is necessary that $F \geq 1$. In particular, $F$ is fundamentally limited by the two-photon absorption component in $\alpha$ given by $\alpha^{(2)}\mathrm{I}$, resulting in an intensity independent contribution to $F$, *i.e.*, its effect cannot be reduced by varying the length of the medium. Recently, Ho *et al.* [42, 45] demonstrated that in AlGaAs the two photon-absorption is drastically reduced in the region below half the energy gap ($\sim$1.6 $\mu$m), enabling the material to meet the figure of merit requirement described above. Another important parameter to consider is the power required to operate the device. For the Mach-Zehnder configuration described in this work, the power required is the power needed to provide a $\pi$ phase shift within the length of the nonlinear medium. For practical applications, it is reasonable to aim for optical peak power in the order of watts, which is the peak power that can be achieved with currently available pulsed semiconductor lasers. In addition, the compactness of a device is another important practical factor and devices with dimensions of the order of centimeters are desirable.

In this Report, we show that by using a 1 cm long microfabricated strongly-guided waveguide with 0.8 $\mu$m by 0.9 $\mu$m fundamental mode cross sectional area, ultrafast all-optical switching can be achieved at a peak power of 30 W, which is not too far from the power requirement for practical applications. We also show that for a conventional 9 mm long rib waveguide with 4.5 $\mu$m by 2.7 $\mu$m mode cross sectional area, switching is achieved at a much higher peak power of 550 W.

The AlGaAs epitaxial layers were grown by MBE and consisted of a $Al_{0.23}Ga_{0.77}As$ guiding region on top of a $Al_{0.60}Ga_{0.40}As$ lower cladding layer grown on a semi-insulating GaAs substrate. The conventional rib waveguide had a 5 $\mu$m thick guiding region, a 2 $\mu$m thick cladding layer, a rib height of 2 $\mu$m and rib width of 4 $\mu$m. The microfabricated waveguide had a 1.5 $\mu$m thick guiding layer, a 2.5 $\mu$m thick lower cladding layer, and its height and width were both around 1.5 $\mu$m. The 9 mm long rib waveguide was fabricated using a conventional photolithography procedure and a chemical etching using $H_3PO_4$:$H_2O_2$:$H_2O$ (1:1:35 volume ratios) as etchant. The 1 cm long microfabricated waveguide was patterned via conventional photolithography, but etched via chemically assisted ion beam etching (CAIBE) with chlorine gas in conjunction with an argon-ion beam. Figure 11 shows a SEM picture of the 1 cm long microfabricated strongly-guided waveguide with 1.5 $\mu$m by 1.5 $\mu$m physical cross sectional area and 0.8 $\mu$m by 0.9 $\mu$m mode cross sectional area. This fabrication procedure gives

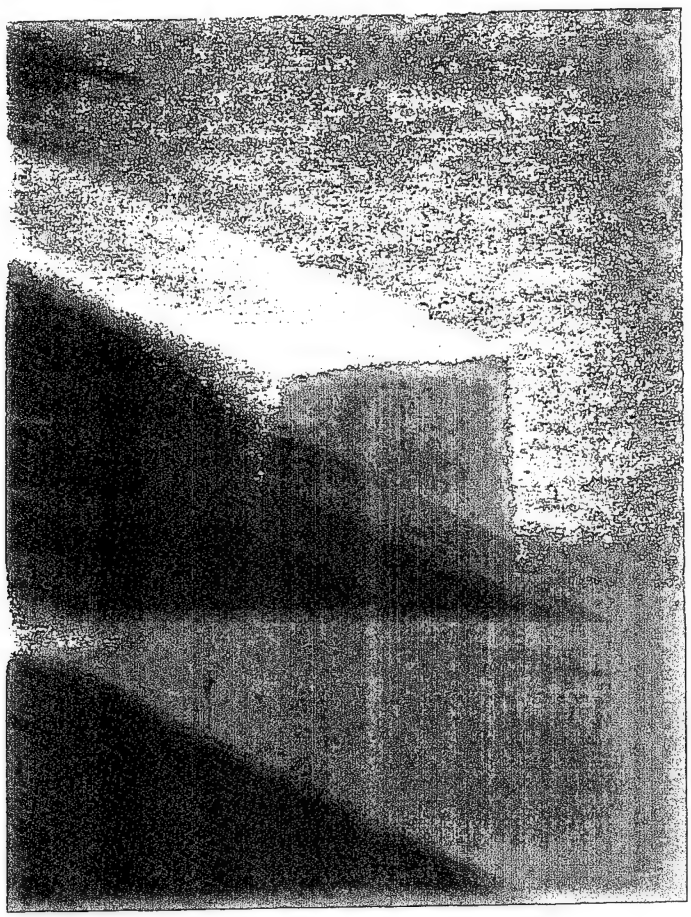

Figure 11: SEM picture of the microfabricated strongly-guided AlGaAs waveguide.

smooth waveguide side walls, which is essential for minimizing waveguide propagation losses.

Figure 12 shows the experimental setup for the all-optical switching using the above described AlGaAs waveguides in the Mach-Zehnder configuration, where the portion comprising the Mach-Zehnder interferometer is indicated by the dotted lines. The details of the all-optical switching experiment are as follows.

An additive pulse mode-locked (APM) color center laser (NaCl:OH) is used to generate high peak intensity pulses with pulse width of 430 fs and a pulse repetition rate of 82 MHz at $\lambda$=1.6 $\mu$m. As shown in Fig. 12, the output of the color center laser is split at the polarization beam splitter PBS1 into a strong pump beam and a weak signal beam with intensity ratio 9 to 1, which can be adjusted by the half-wave plate HWP1. The weak signal beam is further split at PBS2 into $S_{NL}$ and $S_L$ beams which propagate through the nonlinear and linear arms of the Mach-Zehnder interferometer, respectively. Here we refer to the arm containing the AlGaAs waveguide as the nonlinear arm of the interferometer. The orthogonally polarized

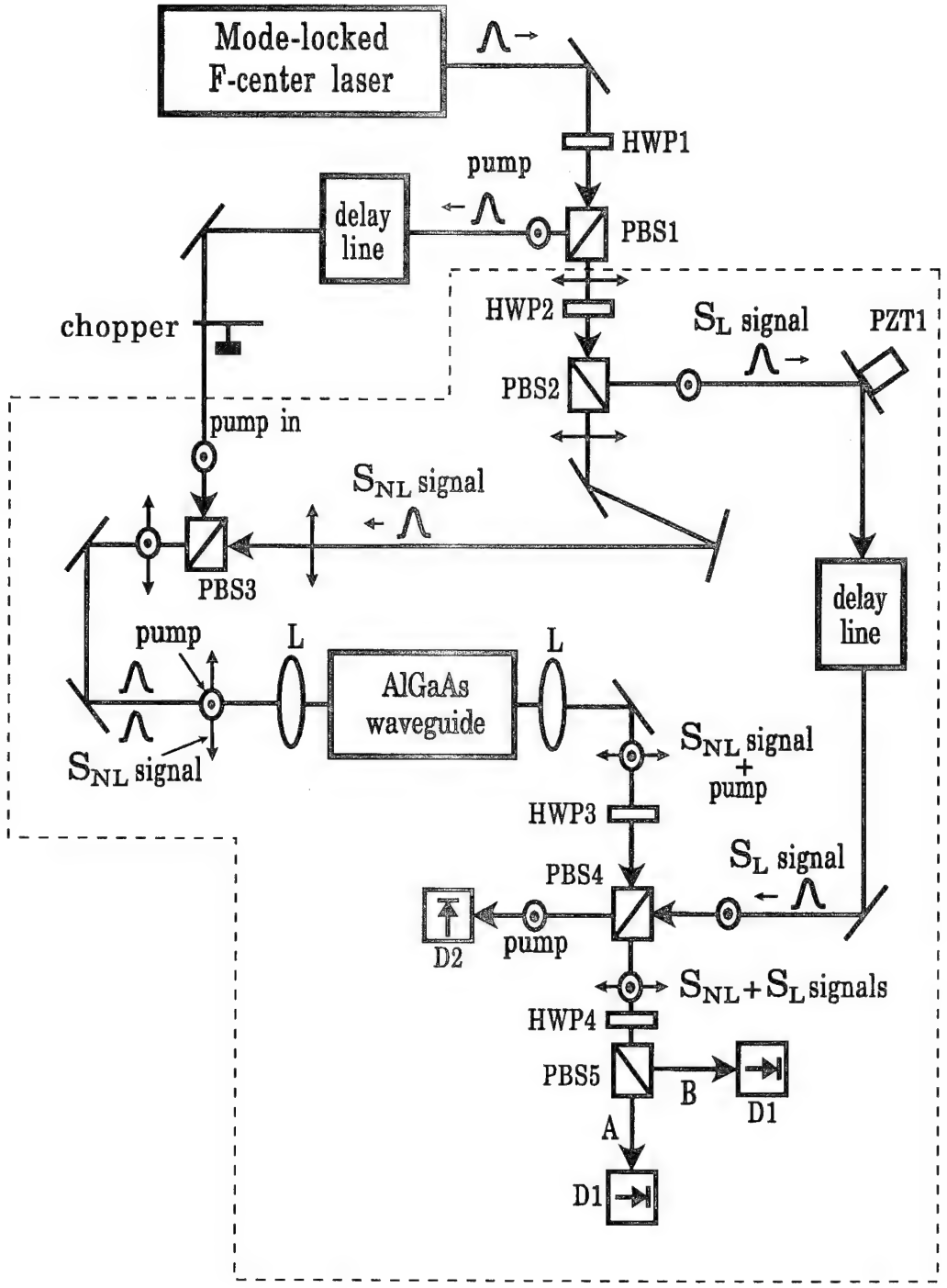


Figure 12: Experimental set up of the Mach-Zehnder configuration for all-optical switching using AlGaAs waveguides.

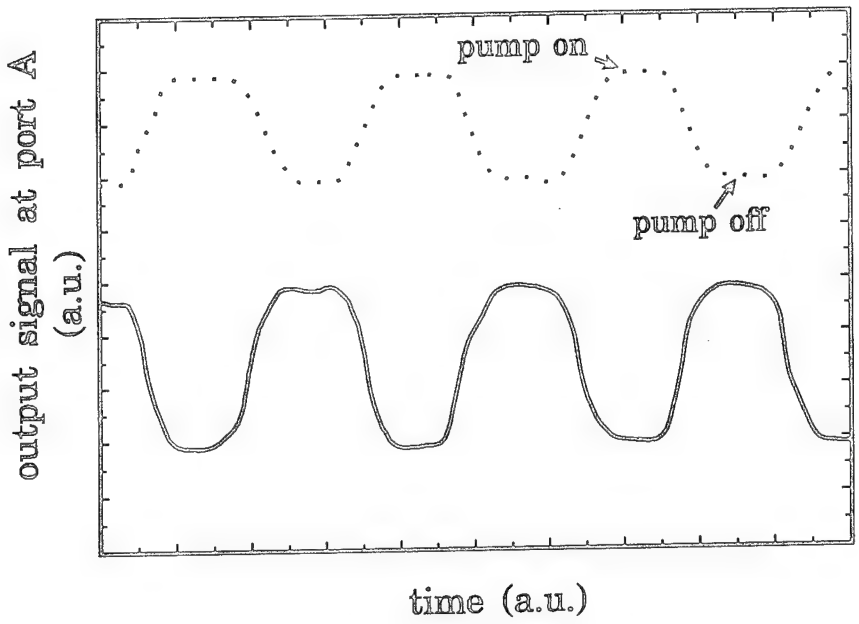


Figure 13: The botton trace (solid curve) shows the modulated output signal at port A of the switch as function of time, while the top trace (dotted line) shows the pump on and off. When the pump is on the output signal increases showing the signal being switched from output port A to B.

pump and $S_{NL}$ signal beams are then combined at the polarization beam splitter PBS3 (i.e. spatially overlapped but still orthogonally polarized) and coupled into the waveguide. The optical coupling into and out of the waveguide was done by the end-firing coupling method using 40x microscope objective lenses with a numerical aperture of 0.6. To minimize losses, both the front and back facets of the waveguide were antireflection coated. After going through the waveguide, the pump beam is separated from the signal beam by the polarization beam splitter PBS4. The pump beam is then detected at detector D2, whose output gives the pump beam intensity after the waveguide. The $S_L$ signal, generated at PBS2, is recombined at the polarization beam splitter PBS4 with the orthogonally polarized $S_{NL}$ signal from the waveguide. The polarizations of $S_L$ and $S_{NL}$ beams after PBS4 are rotated by 45 degrees with a half wave plate (HWP4) and the resulting beam passes through another polarization beam splitter PBS5, where the interference between the $S_L$ and $S_{NL}$ signal beams occurs (the combination of PBS4, HWP4, and PBS5 is equivalent to a polarization insensitive 50/50 beam splitter). The resulting interference signal beam exits at either port A or B of PBS5, depending on whether there is constructive or destructive interference. To demonstrate all-optical switching, the phase of the $S_L$ signal pulse is adjusted by a piezoelectric transducer

(PZT1) and its intensity adjusted by the combination of HWP2 and PBS2 so that in the absence of the strong pump beam, the combined signal pulses exit from port A of PBS5. When the strong pump pulse overlaps the signal pulse inside the waveguide causing a $\pi$ phase shift of the $S_{NL}$ signal pulse via cross-phase modulation, the output signal pulses at PBS5 are switched from port A to port B.

Figure 13 demonstrates ultrafast all-optical switching using the microfabricated AlGaAs waveguide. The interferometer was set so that the output signal at port A has maximum intensity. The solid curve represents the signal at port A of the switch, while the dotted curve shows the pump on and off. When the pump is on the output signal decreases showing the signal being switched from the output port A to B. From the figure we see that there is about 60% switching, limited by the nonlinear cross-phase modulation due to the non-square intensity profile of the pump pulses and by the mode matching efficiency between the interfering signals at PBS5. When the pump and $S_{NL}$ signal pulses in the waveguide are delayed from each other by one or more pulse widths, the amount of switching reduces to zero, demonstrating that the switching speed is faster than 430 fs. From our experimental measurement, we conclude that the $\pi$ nonlinear phase shift needed for optical switching was achieved with a 1.2 mW average power in the waveguide for 82 MHz mode-locked 430 fs pulses at 1.6 $\mu$m wavelength. The estimated peak pump power and pulse energy inside the microfabricated waveguide were ~30 W and ~14.6 pJ, respectively. Currently, the net coupling efficiency in and out of the microfabricated waveguide is about 10%, which could be improved in the future by tapered waveguides or coupling lenses with larger numerical aperture. The propagation loss in the 1 cm long waveguide is estimated to be less than 10% using the cut-back method. For the 9 mm long conventional rib waveguide, switching was achieved with 22 mW average power and the estimated peak power and pulse energy inside the waveguide were ~550 W and ~270 pJ, respectively. Note that the peak pump power necessary for $\pi$ nonlinear phase shift can be smaller by a factor of 2/3 if the pump and probe beams have the same polarization. This is because cross-phase modulation (XPM) is 2/3 as strong as self-phase modulation (SPM) for an isotropic material like AlGaAs [45]. Hence, for the case where the pump and probe beams have the same polarization, the switching peak pump power and pulse energy for the microfabricated waveguide can be reduced to 20 W and 10 pJ, respectively. Since the switching pump power $p$ is inversely proportional to the length of the waveguide $\ell$, the product $p * \ell$ for a given nonlinear waveguide medium is a constant and can be used as a practicality index for the realization of compact ultrafast all-optical switching devices. Based on the discussion in the introductory paragraph, we propose that practical devices should have $p * \ell$ around unity or smaller, where $p$ is in watts and $\ell$ in centimeters. Our microfabricated waveguide, for the case where the pump and

probe beams have the same polarization, has $p * \ell = 20$ W-cm which is lower than the value recently reported for an optical nonlinear directional coupler [46] with $p*\ell = 130$ W-cm (this directional coupler has material composition similar to our waveguide, but larger waveguide mode structure). For comparison purposes, it is useful to note that the $p * \ell$ value for the usual single-mode silica fiber is around 300,000 W-cm. However, optical fibers have the advantage that their lengths can be very long without incurring much loss, while waveguides cannot.

### 4.C.2 Improved Ultrafast All-Optical Switch with Gap Soliton Propagation

We investigated both the theoretical and the experimental aspects of Bragg soliton propagation for all-optical switching applications. In this Report we describe the design, fabrication and characterization of broad band Bragg reflectors in AlGaAs optical waveguides and we also present the results of our theoretical calculations on the propagation of coupled Bragg solitons for all-optical switching applications.

Broad band Bragg reflectors represent an important element for both linear and nonlinear applications. In the linear case, they can be used as filters in wavelength-division multiplexing (WDM) applications, while in the nonlinear case they can be used for nonlinear optical switching. Recently, broad band Bragg reflectors in both polymeric channel waveguides [47] and silica on silicon waveguides [48] have been reported, with reflection bandwidth of 8 nm and 20 nm, respectively. We now describe the fabrication and characterization of broad band Bragg reflectors in micro-fabricated AlGaAs optical waveguides. These Bragg reflectors exhibited a maximum FWHM reflection band of about 15nm centered about 1.6 $\mu$m with a reflectivity of over 90%.

Bragg reflectors in waveguides are characterized by the center wavelength and bandwidth of the reflection band. The center wavelength of the reflector is determined by the period of the Bragg gratings via the relation $\lambda_B = 2n_{eff}\Lambda$, where $\lambda_B$ is the center wavelength of the reflector, $n_{eff}$ is the effective refractive index of the guided mode, and $\Lambda$ is the period of the Bragg gratings. In this description we assume only first-order Bragg gratings and a guided-mode propagation in the direction perpendicular to the gratings. The bandwidth of the Bragg reflector $\Delta\lambda$ is proportional to the effective refractive index modulation $\Delta n_{eff}$ and can be shown to be approximately given by[6] $\Delta\lambda/\lambda \sim \Delta n_{eff}/n_{eff}$, where this relation is stricly valid only when $\Delta n_{eff} << n_{eff}$. As can be seen from the last relation, broad band Bragg reflectors require a sizable $\Delta n_{eff}$. For example, a Bragg reflector with a 10 nm bandwidth at 1.6 $\mu$m requires about a 0.6% refractive index modulation. The large index modulation in waveguides can only be obtained by fabricating relatively deep gratings on the guiding layer.

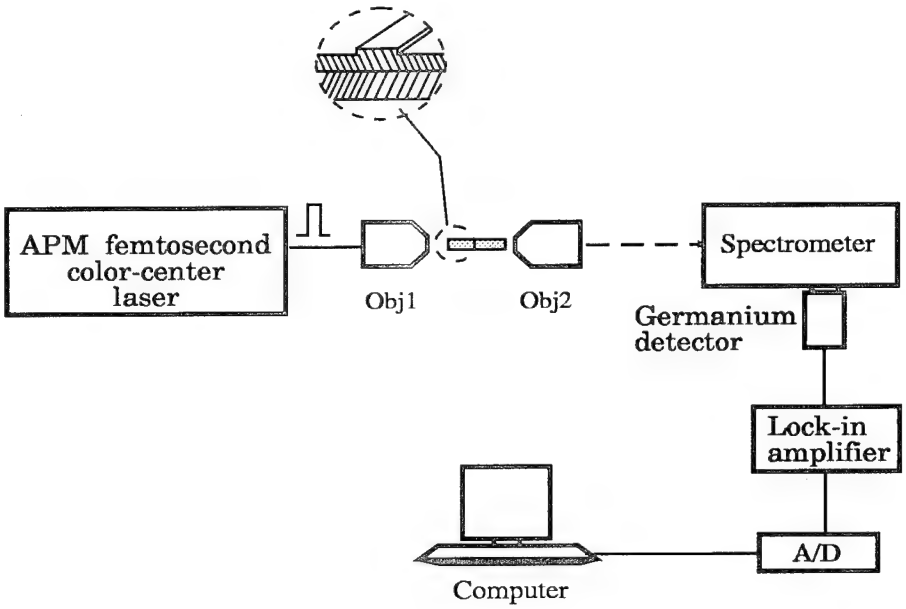


Figure 14: Experimental set up for measuring the Bragg reflector bandwidth.

The AlGaAs Bragg reflector waveguides were fabricated using a multi-step photolithographic technique, by first fabricating the gratings and then the waveguides. The AlGaAs wafer was first coated with polymethylmethacrylate (PMMA) resist and then baked at 170°C for one hour. A 0.8mm long grating pattern was then written on the PMMA using a JEOL JBX 5DIIU electron beam system and after the appropriate processing the PMMA was developed. The resist image was then transferred to the AlGaAs wafer by chemically assisted ion-beam etching (CAIBE) using chlorine gas in conjunction with argon ion beam. The PMMA resist was then stripped using the appropriate solvents and the resulting grating was measured to have a depth of about 0.3$\mu$m. After the grating fabrication, waveguides were patterned perpendicular to the gratings and etched down the cladding to form strongly-guided one-dimensional optical waveguides. The waveguides were 1.5$\mu$m wide, 1 mm long and there was a 0.1 mm waveguiding region between the input of the waveguide and the beginning of the Bragg reflector.

The bandwidth of the Bragg reflectors was determined by coupling spectrally broad femtosecond pulses into the waveguides and measuring the transmitted pulse spectrum. A schematic of the experimental setup is shown in Fig. 14. The laser source used in this experiment is the same as described in the previous section, but with 150 fs pulses. The bandwidth of the 150 fs pulses was measured to be 18.2 nm using a spectrometer, giving a time-bandwidth product of about 0.32. This value is close to the transform limit of 0.315 for $\text{sech}^2$ pulse envelope. The pulse center wavelength was set using a birefringent filter at about

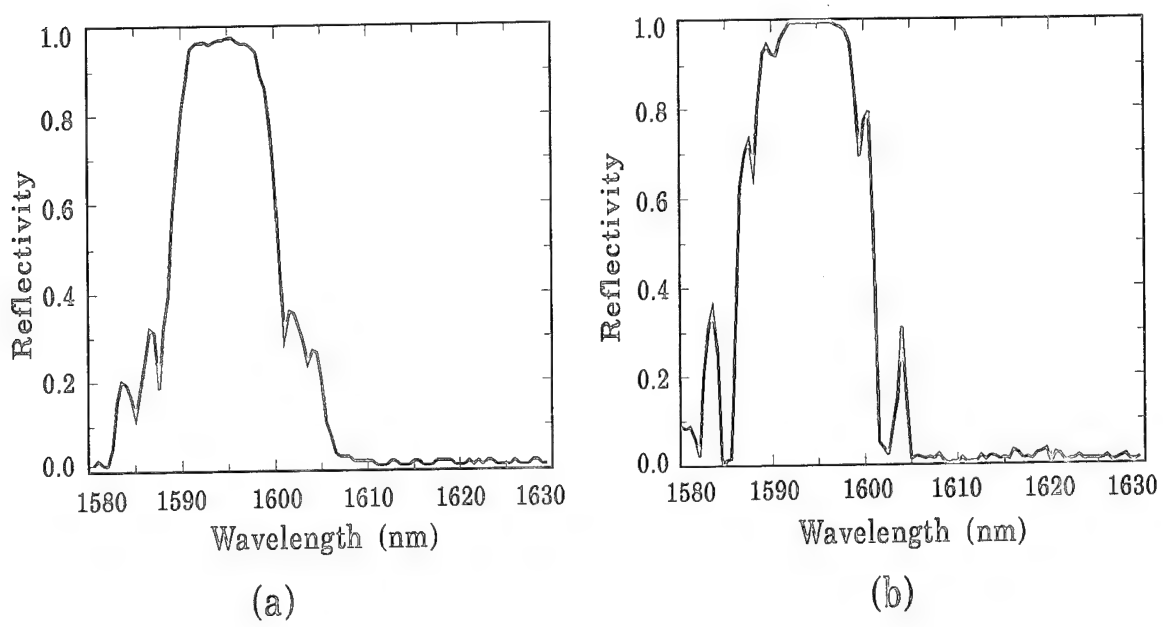


Figure 15: Reflectivity espectrum as function of wavelength for: (a) 1.2$\mu$m thick Bragg reflector waveguide, and (b) 1.0 $\mu$m thick Bragg reflector waveguide.

1.6$\mu$m in order to coincide with the center wavelength of the Bragg reflector. The pulses were coupled into the waveguide by the end-firing method using 40x microscope objective lenses with a 0.6 numerical aperture. By a careful alignment of the input beam, only the lowest order mode of the waveguide was excited. To minimize losses both the front and back facets of the waveguide were antireflection coated. The transmitted spectrum was measured using a computer controlled Spex 270M scanning spectrometer (maximum resolution of 0.1 nm) together with a liquid nitrogen cooled germanium detector and a lock-in amplifier. The power coupled into the waveguide was sufficiently low to minimize self-phase modulation of the transmitted pulses.

Figure 15(a) shows the reflectivity spectrum versus wavelength for the 1.2 $\mu$m thick Bragg reflector waveguide. The reflectivity spectrum was obained by normalizing the transmitted pulse spectrum with the input pulse spectrum. As can be seen from the figure, the reflectivity spectrum is centered at 1595 nm, has a FWHM bandwidth of about 11 nm, and has maximum reflectivity of about 95%. Figure 15(b) shows the reflectivity spectrum versus wavelength for the 1.0 $\mu$m thick Bragg reflector waveguide. For this case, the reflectivity spectrum is centered at about 1593 nm, has a bandwidth of about 15 nm, and has maximum reflectivity of 98%.

The above described grating structures were used to experimentally investigate Bragg soliton propagation. In performing this experiment we found that the pulse intensity of our color center laser was not high enough to propagate Bragg solitons due to optical coupling

and propagation losses. To obtain higher intensity pulses, we built an optical amplifier system that allows us to amplify the intensity of the color center laser pulses by a factor of 100 or better. In addition to the pulse intensity needed we found that pico-second pulses were more appropriate for this experiment than femtosecond pulses. Our initial trials, however, indicate that multi-photon absorption could be substantial at the power region for the formation of gap solitons and may impose a problem.

As part of this task we also performed some theoretical studies and found that Bragg solitons can have potential use in realizing all-optical switches. According to our recent theoretical calculations, we find that due to cross-coupling $\chi^{(3)}$ between pulses of different polarizations in a nonlinear optical waveguide, two orthogonally polarized pulses can co-propagate through a nonlinear periodic grating waveguide structure as coupled Bragg solitons provided their intensities are high enough. It turns out that the intensity of each pulse needed to propagate coupled Bragg solitons is lower than that needed to propagate one single Bragg soliton. Thus, if one pulse is blocked, then the other pulse will not be able to go through the grating. This scheme could allow us to use one pulse to control the other pulse, thereby achieving all-optical switching.

### 4.C.3 Single-Quadrature Duplicator

We performed a theoretical investigation to examine in detail the feasibility of using a short AlGaAs semiconductor waveguide with $\chi^{(3)}$-nonlinearity [45] to generate squeezing. Compared with fiber, the unique feature of the AlGaAs semiconductor waveguide is that substantial amount of squeezing can be achieved in centimeter-long AlGaAs semiconductor waveguides with negligible guided acoustic-wave Brillouin scattering noise (GAWBS noise) [49]. This makes it possible to build a compact and simple scheme with AlGaAs semiconductor waveguide to generate squeezing. It tuns out that with the same pump power, the waveguide length needed to generate large amounts of squeezing in an AlGaAs semiconductor waveguide is approximately $10^4$ times less than that in a silica fiber. The reason is two-fold. First, the nonlinear four-wave mixing gain coefficient of AlGaAs is 100 times that of typical optical fibers. Second, the mode cross-sectional area of a single-mode AlGaAs rib waveguide is approximately 100 times smaller than that of a single-mode fiber. The much smaller cross-sectional area is because of a higher material refractive index and stronger optical confinement found in AlGaAs semiconductor waveguides compared to optical fibers. Because of the short length of the semiconductor waveguide, GAWBS noise will be negligible. This eliminates the additional apparatus and techniques needed to combat GAWBS noise and further simplifies the experimental set up for generating squeezing in semiconductor waveguides.

Our theoretical analysis takes into account the various effects that potentially limit the

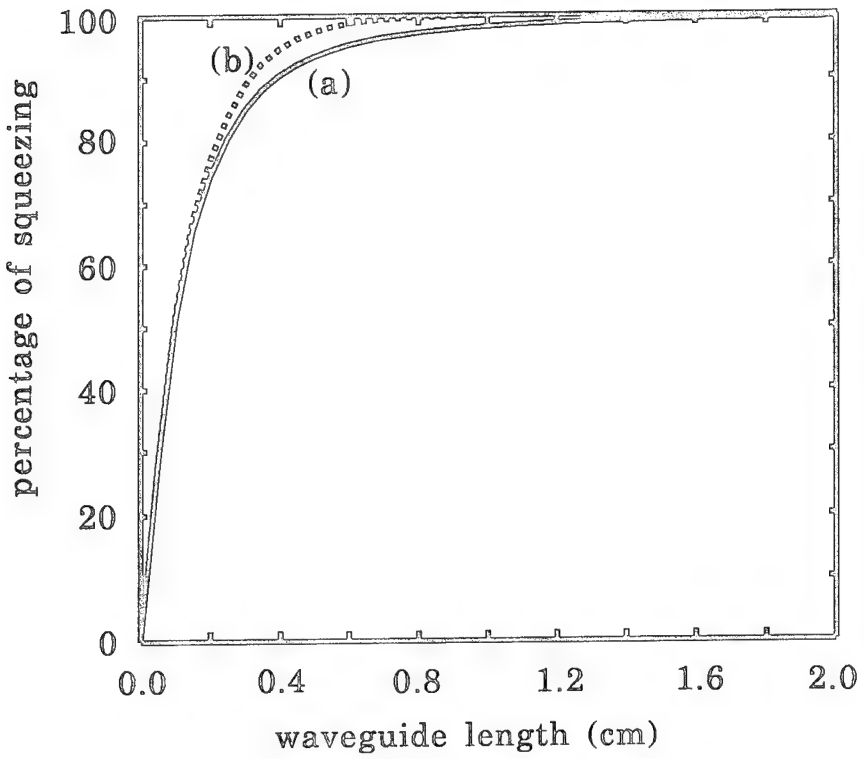


Figure 16: The effect of nonlinear pump-probe phase mismatch $\Delta\kappa$ on the amount of squeezing, as function of waveguide length for a square pump pulse, uniform phase LO and without nonlinear absorption: (a) $\Delta\kappa \neq 0$, and (b) $\Delta\kappa = 0$.

amount of squeezing achievable. They include: (i) nonlinear pump-probe phase mismatch, (ii) nonlinear absorption, and (iii) squeezed-state detection (SSD) phase mismatch. The effects of pump-probe phase mismatch and nonlinear absorption exist for any type of pump pulses including CW pump. The effect of SSD phase mismatch is present for either Gaussian pulses or any other pulses without uniform intensity profile when a uniform-phase local oscillator (LO) pulse is used. We now present the results of our numerical analysis when these three effects are included. In our calculations we used the parameters for AlGaAs as given in Ref. [45]. These are, for AlGaAs waveguide at wavelength $\lambda$=1.55$\mu$m, two-photon absorption coefficient $\alpha^{(2)}$=0.26$\times 10^{-4}$cm/MW, three-photon absorption coefficient $\alpha^{(3)}$=(3.6$\pm$0.5)$\times 10^{-14}$cm$^2$/W. When the pump and probe beams have the same polarization, $\kappa_s = (4\pi/\lambda)n^{(2)}$ and $\gamma = 2(\alpha^{(2)} + \alpha^{(3)} I_p) I_p$. In all the calculations we choose a typical pump pulse peak intensity of $4.5 GW/cm^2$, which can be achieved in a laboratory.

We first present the case in which the nonlinear absorption is neglected. To see the effect of pump-probe phase mismatch $\Delta\kappa$ only, we choose a square pulse as the pump pulse because it does not have SSD phase mismatch. Figure 16 shows the results of our numerical calculations, with curve (a) describing the effect of pump-probe phase mismatch, while in

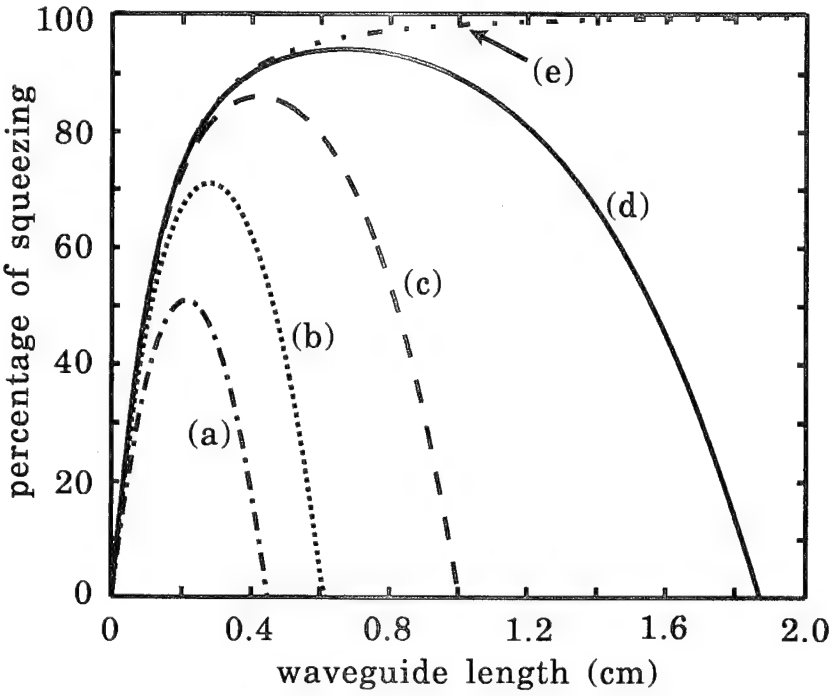


Figure 17: Effect of SSD phase mismatch on squeezing for a Gaussian pump pulse with uniform phase under its pulse profile and without nonlinear absorptio: (a) LO pulse has the same width as the Gaussian pump pulse; (b), (c), and (d) narrow uniform-phase LO pulse, where the LO pulse width is taken to be 1/2, 1/4, and 1/8 of that of the pump pulse, respectively. Curve (e) illustrates the square pump pulse case as a comparison.

curve (b) $\Delta\kappa$ was set to zero.

Comparing these two curves, one can see that in the short waveguide region the amount of squeezing is reduced by less than 5% due to pump-probe phase mismatch, while for long waveguide length the maximum amount of squeezing approaches 100% on both cases with no apparent difference between them. Hence, the pump-probe phase mismatch reduces the effective interaction strength but does not limit the amount of squeezing achievable.

We now present the results on the amount of squeezing achievable using a Gaussian pump pulse, which describes more closely the pulses obtained experimentally in the laboratory. As mentioned earlier, a Gaussian pump pulse with a uniform-phase LO pulse will result in SSD phase mismatch. To take into account the effect of SSD phase mismatch, our numerical analysis was carried out by dividing the Gaussian pulse into many slices, and each slice was approximated by a square pulse. We first consider the case in which the LO pulse is also chosen to be a Gaussian pulse with the same pulse width as the pump, but with uniform

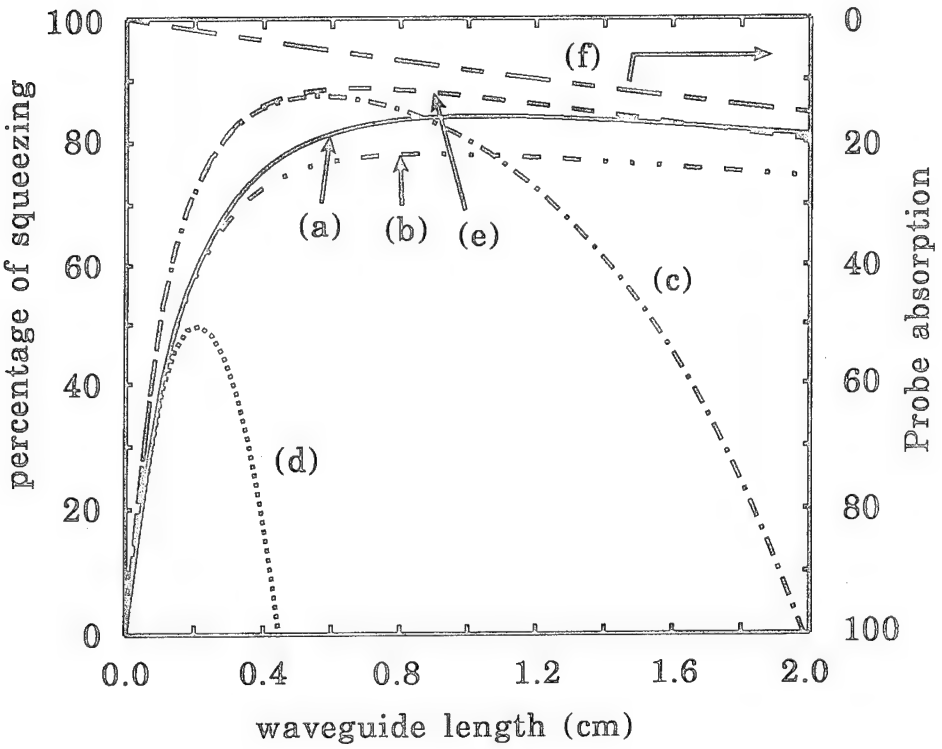


Figure 18: Squeezing with nonlinear absorption: (a) Gaussian pump pulse with nearly matched LO pulse from another waveguide; (b) Gaussian pump pulse with reused pump pulse; (c) Gaussian pump pulse with narrower uniform-phase LO pulse; (d) Gaussian pump pulse with uniform-phase LO having the same width as the pump; (e) Square pump pulse; (f) Relative pump amplitude $E_p(l)/E_p(0)$.

phase $\phi$. The maximum amount of squeezing achievable as function of waveguide length is obtained by varying the LO phase. Figure 17 shows that in this case the maximum amount of squeezing achievable is about 50% as illustrated by curve 17(a), and as the waveguide length increases, the effect of SSD phase mismatch is so strong that the amount of squeezing goes to zero. By choosing either a narrow or a matched LO pulse it is possible to improve the amount of squeezing achievable. We repeated our calculation using a narrow LO pulse with pulse width narrower than that of squeezed vacuum pulse and overlap the center of the LO pulse with that of the squeezed vacuum pulse. In this case, the SSD phase matching condition can be satisfied in the neighborhood of the pulse center. Squeezing will be detected in this region and noise will be ignored at all other places. Curves 8(b), 8(c), and 8(d) show the results for a uniform-phase Gaussian LO pulse with a pulse width 1/2, 1/4, and 1/8 of that of the Gaussian pump pulse, respectively. In the case illustrated by curve 8(d), we see that for short waveguide length the maximum amount of squeezing is close to 95%, approaching

the ideal square pump pulse case, which is illustrated in curve 7(a). For long propagation medium length, the amount of squeezing decreases, departing from the asymptote observed for the square pulse case, possibly due to the fact that the LO pulse begins to pick up the anti-squeezed components as the pump undergoes further self-phase modulation. We also investigated the effect of nonlinear absorption on the amount of squeezing achievable. For very small nonlinear absorption, which corresponds to a $\chi^{(3)}$-medium with small nonlinear absorption coefficient or relatively short $\chi^{(3)}$-medium, the results are illustrated in Figure 18. Figure 18(a)-18(d) are results of Gaussian pump pulse with different LO pulse. Figure 18(a) is for the nearly matched LO pulse. In Fig. 18(b), LO pulse is reused pump pulse. In Fig. 18(c), LO pulse is a uniform-phase Gaussian pulse with pulse width narrower than that of the pump pulse (1.8 the pump pulse width). In Fig. 18(d), LO pulse is simply a Gaussian pulse with uniform phase and same pulse width as the pump pulse. Figure 18(e) is the result of a square pump pulse. We see that even with nonlinear absorption included, for the case of a Gaussiam pump pulse about 85% squeezing can be achieved when a narrow or nearly-matched LO pulse is used.

For the experimental observation of squeezed state generation we have fabricated waveguides using AlGaAs grown by MBE, as described in Section 3.1 of this report. We obtained some initial results indicating classical noise squeezing. The noise level was still too high to observe quantum noise squeezing. The difficulties with the noise level were traced to the detection system and also to our mode-locked femtosecond laser pulses.

# 5 References


[1] H. P. Yuen, "Nonclassical Light," in *Photons and Quantum Fluctuations*, ed. by E. R. Pike and H. Walther, Adam Hilger, 1988, pp. 1-9.

[2] H. P. Yuen, "Reduction of Quantum Fluctuation and Suppression of Gordon-Haus Effect in Phase-Sensitive Linear Amplifiers," Opt. Lett. vol. 17, 1992, pp. 73–75.

[3] O. Aytür and P. Kumar, "Pulsed Twin Beams of Light," Phys. Rev. Lett. vol. 65, 1990, pp. 1551-1554.

[4] L. F. Mollenauer, P. V. Mamyshev, and M. J. Neubelt, "Measurement of timing jitter in filter-guided soliton transmission at 10 Gbits/s and achievement of 375 Gbits/s-Mm, error free, at 12.5 and 15 Gbits/s," Opt. Lett., vol. 19, 1994, pp. 704-706.

[5] J. P. Gordon and L. F. Mollenauer, "Effects of Fiber Nonlinearities and Amplifier Spacing on Ultra-Long Distance Transmission," J. Lightwave Tech. vol. 9, 1991, pp. 170-173.

[6] J. P. Gordon and H. A Haus, "Random Walk of Coherently Amplified Solutions in Optical Fiber Transmission", Opt. Lett., vol. 11, 1986, pp. 665-667.

[7] H. P. Yuen, "Generation, Detection and Application of High-Intensity Photo-Number-Eigenstate Fields," Phys. Rev. Lett., vol. 56, 1986, pp. 2176-2179.

[8] S. S. Wagner, "Optical Amplifier Applications in Fiber Optic Local Networks," IEEE Transactions on Communications, vol. COM-35, 1987, pp. 419-426.

[9] H. P. Yuen, "Design of Transparent Optical Networks by Using Novel Quantum Amplifiers and Sources," Opt. Lett., vol. 12, 1987, pp. 789-791.

[10] H. P. Yuen, "Photon Number Duplication and Quantum Nondemolition Detection," in *Quantum Aspects of Optical Communications*, C. Bendjaballah, O. Hirota, and S. Reynaud, Eds. Lecture Notes in Physics, Vol. 378 (Springer, Berlin, 1991), pp. 333.

[11] V. Mizrahi, K. W. DeLong, G. I. Stegeman, M. A. Saifi and M. J. Andrejco, "Two-photon absorption as a limitation to all-optical switching," Opt. Lett., vol. 14, 1989, pp. 1140-1142.

[12] M. N. Islam, C. E. Soccolich, C. J. Chen, K. S. Kim, J. R. Simpson, and U. C. Paek, "All-optical inverter with 1 pJ Switching Energy," Conference on Lasers and Electro-Optics, 1991 Technical Digest Series Volume 10, CMB3, pp. 18.

[13] C. Martijn de Sterke and J. E. Sipe, "Self-localized light: launching of low-velocity solitons in corrugated nonlinear waveguides," Opt. Lett., vol. 16, 1989, pp. 871-873.

[14] S.-T. Ho and H. P. Yuen, "Scheme for realizing a photon number amplifier," Opt. Lett., vol. 19, 1994, pp. 61.

[15] H. P. Yuen and M. Ozawa, "Ultimate information carrying limit of quantum systems," Phys. Rev. Lett., vol. 70, 1993, pp. 363.

[16] L. F. Mollenauer, M. J. Neubelt, S. G. Evangelides, J. P. Gordon, J. R. Simpson, and L. G. Cohen, "Experimental study of soliton transmission over more that 10,000 km in dispersion-shifted fiber," Opt. Lett., vol. 15, 1990, pp. 1203-1205.

[17] J. N. Kutz, W. L. Kath, R.-D. Li, and P. Kumar, "Long-distance pulse propagation in nonlinear optical fibers using periodically-spaced parametric amplifiers," Opt. Lett., vol. 18, 1993, pp. 802.

[18] J. N. Kutz, C. V. Hile, W. L. Kath, R.-D. Li, and P. Kumar, "Pulse propagation in nonlinear optical fiber-lines that employ phase-sensitive parametric amplifiers," J. Opt. Soc. Am. B vol. 19, 1994, pp. 2050.

[19] A. Mecozzi, W. L. Kath, P. Kumar, and C. G. Goedde, "Long-term storage of a soliton bit stream using phase-sentitive amplification," Opt. Lett., vol. 11, 1994, pp. 2112.

[20] N. S. Bergano, J. Aspell, C. R. Davidson, P. R. Trischitta, B. M. Nyman, and F. W. Kerfoot, "Bit error-rate measurements of 14,000 km 5 Gb/sec fiber-amplifier transmission system using circulating loop," Electron. Lett. vol. 27, 1991, pp. 1889-1890.

[21] A. Hasegawa and Y. Kodama, "Guiding-center soliton in optical fibers",. Opt. Lett., vol. 15, 1990, pp. 1443–1445; "Guiding-center soliton", Phys. Rev. Lett., vol. 66, 1991, pp. 161–164. Y. Kodama and A. Hasegawa, "Theoretical foundations of optical-soliton concept in fibers", in *Progress in Optics XXX*, E. Wolf, ed., (Elsevier, Amsterdam, 1992).

[22] L. F. Mollenauer, S. G. Evangelides and H. A. Haus, "Long-distance soliton propagation using lumped amplifiers and dispersion shifted fiber", J. Lightwave Tech. vol. 9, 1991, pp. 194–197.

[23] A. Mecozzi, J. D. Moores, H. A. Haus and Y. Lai, "Soliton transmission control", Opt. Lett., vol. 16, 1991, pp. 1841–1843; Y. Kodama and A. Hasegawa, "Generation of asymptotically stable optical solitons and suppression of the Gordon-Haus effect", Opt.

Lett., vol. 17, 1992, pp. 31–33; L. F. Mollenauer, J. P. Gordon and S. G. Evangelides, "The sliding-frequency guiding filter: an improved form of soliton jitter control", Opt. Lett., vol. 17, 1992, pp. 1575–1577.

[24] E. M. Dianov, A. V. Luchnikov, A. N. Pilipetskii, and A. N. Starodumov, "Electrostriction mechanism of soliton interaction in optical fibers", Optics Letters, vol. 15, 1990, pp. 314–316; "Long-range interaction of solitons in ultra-long communication systems", Soviet Lightwave Comm. vol. 1, 1991, pp. 235-246.

[25] H. Yuen, "Reduction of quantum fluctuation and suppression of the Gordon-Haus effect with phase-sensitive linear amplifiers", Opt. Lett., vol. 17, 1992, pp. 73–75.

[26] Sueng-Hee Lee, "Ultra-long distance optical communication using phase-sensitive linear amplifier chains", Ph.D. Thesis, Northwestern University, December 1992.

[27] R.-D. Li, P. Kumar, W. L. Kath, and J. N. Kutz, "Combating dispersion with parametric amplifiers," IEEE Photon. Technol. Lett., vol. 5, 1993, pp. 669–672.

[28] R.-D. Li, P. Kumar and W. L. Kath, "Dispersion compensation with phase-sensitive amplifiers", J. of Lightwave Technol. vol. 12, 1994, pp. 541–549.

[29] P. S. Henry, "Lightwave primer," IEEE J. Quantum Electron., vol. QE-21, 1985, pp. 1862–1879.

[30] G. P. Agrawal, *Nonlinear Fiber Optics*, (Academic Press, New York, 1989), Chaps. 1 and 3.

[31] A. Hasegawa and F. Tappert, "Transmission of stationary nonlinear optical pulses in dispersive dielectric fibers," Appl. Phys. Lett., vol. 23, 1973, pp. 142–144;
L. F. Mollenauer, R. H. Stolen, and J. P. Gordon, "Experimental observation of picosecond pulse narrowing and solitons in optical fibers," Phys. Rev. Lett., vol. 45, 1980, pp. 1095–1097;
L. F. Mollenauer, R. H. Stolen, and M. N. Islam, "Experimental demonstration of soliton propagation in long fibers: Loss compensation by Raman Gain," Opt. Lett., vol. 10, 1985, pp. 229–231.

[32] Y.-K. Chen and M. C. Wu, "Monolithic colliding-pulse mode-locked quantum-well lasers," IEEE J. Quantum Electron., vol. QE-28, 1992, pp. 2176–2185.

[33] F. Ouellette, "Dispersion cancellation using linearly chirped Bragg grating filters in optical waveguides," Opt. Lett., vol. 12, 1987, pp. 847–849.

[34] L. J. Cimini, Jr., L. J. Greenstein, and A. A. M. Saleh, "Optical equalization to combat the effects of laser chirp and fiber dispersion," J. Lightwave Technol., vol. 8, 1990, pp. 649–659.

[35] A. D. Ellis, S. J. Pycock, D. A. Cleland, and C. H. F. Sturrock, "Dispersion compensation in 450 km transmission system employing standard fiber," Electron. Lett., vol. 28, 1992, pp. 954–955.

[36] H. Izadpanah, C. Lin, J. L. Gimlett, A. J. Antos, D. W. Hall, and D. K. Smith, "Dispersion compensation in 1310 nm-optimized SMFs using optical equalizer fiber, EDFAs and 1310/1550 nm WDM," Electron. Lett., vol. 28, 1992, pp. 1469–1471.

[37] A. Yariv, D. Fekete, and D. M. Pepper, "Compensation for channel dispersion by nonlinear optical phase conjugation," Opt. Lett., vol. 4, 1979, pp. 52–54.

[38] S. Watanabe, T. Naito, and T. Chikama, "Compensation of chromatic dispersion in a single-mode fiber by optical phase conjugation," IEEE Photon. Technol. Lett., vol. 5, 1993, pp. 92–95.

[39] C. D. Poole, J. M. Wiesenfeld, A. R. McCormick, and K. T. Nelson, "Broadband dispersion compensation by using the higher-order spatial mode in a two-mode fiber," Opt. Lett., vol. 17, 1992, pp. 985–987.

[40] M. E. Marhic and C.-H. Hsia, "Optical amplification in a nonlinear interferometer," Elect. Lett. vol. 27, 1991, pp. 210.

[41] G. Bartolini, R.-D. Li, P. Kumar, W. Riha, and K. V. Reddy, "1.5 $\mu$m phase-sensitive amplifier for high-speed communications," OFC'94 Technical Digest, Vol. 4, (Optical Society of America, Washington, D.C., 1994), pp. 202–203.

[42] A. Villeneuve, C. C. Yang, P. G. Wigley, G. I. Stegeman, J. S. Aitchinson, and C. N. Ironside, "Ultrafast all-optical switching in semiconductor nonlinear directional-couplers at half the band-gap," Appl. Phys. Lett., vol. 61, 1992, pp. 147-149.

[43] K. Al-hemyari, J. S. Aitchison, C. N. Ironside, G. T. Kennedy, R. S. Grant, and W. Sibbett, "Ultrafast all-optical switching in GaAlAs integrated interferometer in 1.55 $\mu$m spectral region," Electron. Lett., vol. 28, 1992, pp. 1090-1092.

[44] M. N. Islam, C. E. Soccolich, R. E. Slusher, A. F. J. Levi, W. S. Hobson, and M. G. Young, "Nonlinear spectroscopy near half-gap in bulk and quantum-well GaAs/AlGaAs wave-guides," J. Appl. Phys., vol. 71, 1992, pp. 1927-1935.

[45] S. T. Ho, C. E. Soccolich, M. N. Islam, W. S. Hobson, A. F. J. Levi, and R. E. Slusher, "Large nonlinear phase-shifts in low-loss $Al_xGa_{1-x}As$ wave-guides near 1/2-gap," Appl. Phys. Lett., vol. 59, 1991, pp. 2558-2560.

[46] K. Al-hemyari, A. Villeneuve, J. U. Kang, J. S. Aitchison, C. N. Ironside, and G. I. Stegeman, "Ultrafast all-optical switching in GaAlAs directional-couplers at 1.55 $\mu$m without multiphoton absorption," Appl. Phys. Lett., vol. 63, 1994, pp. 3562-3564.

[47] S. Aramaki, G. Assanto, G. I. Stegeman, W. H. G. Horstuis, and G. Mohlman, "Integrated Bragg reflectors in polymeric channel waveguides," Opt. Comm., vol. 94, 1992, pp. 326-330.

[48] R. Adar, C. H. Henry, R. C. Kistler, R. F. Kazarinov, and J. S. Weiner, "Wide-band Bragg reflectors made with silica on silicon waveguides," Appl. Phys. Lett., vol. 60, 1992, pp. 1924-1926.

[49] R. M. Shelby, M. D. Levenson, and P. W. Bayer, "Guided acoustic-wave Brillouin scattering," Phys. Rev. B, vol. 31, 1985, pp. 5244.

# 6 List of Journal Publications Resulting from this Contract

1. S.-T. Ho and H. P. Yuen, "Scheme for realizing a photon number amplifier," Opt. Lett., vol. 19, 1994, pp. 61-63.

2. H. P. Yuen and M. Ozawa, "Ultimate information carrying limit of quantum systems," Phys. Rev. Lett., vol. 70, 1993, pp. 363-366.

3. "Combating dispersion with parametric amplifiers," (with R.-D. Li, W. L. Kath, and J. N. Kutz), IEEE Photonics Techonology Letters, Vol. 5, 1993, pp. 669–672.

4. "Dispersion compensation with phase-sensitive optical amplifiers," (with R.-D. Li and W. L. Kath), J. Lightwave Technology, vol. 12, 1994, pp. 541–549.

5. "Long-distance pulse propagation in nonlinear optical fibers by using periodically spaced parametric amplifiers," (with J. N. Kutz, W. L. Kath, and R.-D. Li), Opt. Lett., vol. 18, 1993, pp. 802-804.

6. "Pulse propagation in nonlinear optical-fiber lines that employ phase-sensitive parametric amplifiers," (with J. N. Kutz, C. V. Hile, W. L. Kath, and R.-D. Li), J. Opt. Soc. Am. B, vol. 11, No. 10, 1994, pp. 2112–2123.

7. "1.5 $\mu$m phase-sensitive amplifier for high-speed communications," (with G. Bartolini, R.-D. Li, W. Riha, and K. V. Reddy), presented at the 1994 Optical Fiber Communications Conference (OFC'94), held in San Jose, California, February 20–25. See OFC'94 Technical Digest, Vol. 4, (Optical Society of America, Washington, D.C., 1994), pp. 202–203.

8. "Long-term storage of a soliton bit stream using phase-sensitive amplification," (with A. Mecozzi, W. L. Kath, and C. G. Goedde) to appear in Opt. Lett..

9. "Phase Sensitive Amplifiers for Ultra-long Distance Soliton Propagation," (with W. L. Kath, J. N. Kutz, and R.-D. Li), in Optics in 1993, Optics & Photonics News, Vol. 4, No. 12, 1993, pp. 11.

10. S. Lee and S. T. Ho, "Optical Switching Scheme Based on the Transmission of Coupled Gap Solitons in Nonlinear Periodic Dielectric Media," Opt. Lett., vol. 18, 1993, pp. 962-964.

11. R. P. Espindola, M. K. Udo, D. Y. Chu, S. L. Wu, R. C. Tiberio, P. F. Chapman, D. Cohen, and S. T. Ho, "All-optical switching with low peak power in microfabricated AlGaAs waveguides," accepted for publication in Photonics Technology Letters.

12. S. T. Ho, X. Zhang, and M. K. Udo, "Single-Beam Squeezed-State Generation in Semiconductor Waveguides with $\chi^{(3)}$ Nonlinearity," accepted for publication in the J. Opt. Soc. Am. B.

13. R. P. Espindola, M. K. Udo, and S. T. Ho, "Single-beam Nearly-Degenerate Frequency Technique for Waveguide Measurement of Electronic $n^{(2)}$, thermal $n^{(2)}$, $\alpha^{(2)}$, and Four-Wave Mixing Gain Coefficients," submitted to Opt. Comm.

14. R. P. Espindola, M. K. Udo, D. Y. Chu, S. L. Wu, R. Tiberio, P. Chapman, and S. T. Ho, "Broadband Bragg Reflector in Nonlinear Semiconductor Optical Waveguides for Soliton and WDM Applications," to be submitted to App. Phys. Lett.

15. R. P. Espindola, M. K. Udo, D. Y. Chu, S. L. Wu, and S. T. Ho, "Parametric Amplification of Femtosecond Pulses at 1.55$\mu$m in AlGaAs Waveguides using a Novel Single-pass Single-beam Pulsed-delayed Scheme," to be submitted to Opt. Lett.

# 7 List of Conference Presentations Resulting from this Contract

1. "Degenerate four-wave mixing noise measurements in semiconductors," (with D. Caplan), presented at the 1994 Optical Society of America Annual Meeting, Dallas, Texas, October 2–7, 1994. See Supplement to *Optics and Photonics News*, Vol. 5, No. 8, August 1994, pp. 126.

2. "Optical pulse shaping using phase-sensitive amplification," (with W. L. Kath and J. E. Oleksy), presented at the 1994 Integrated Photonics Research Conference (IPR'94), San Francisco, California, February 17–19, 1994. See IPR'94 Technical Digest, Vol. 3, (Optical Society of America, Washington, D.C., 1994), pp. 319–321.

3. "Phase-sensitive optical amplifiers," (with W. L. Kath and R.-D. Li), **invited paper** presented at the 1994 Integrated Photonics Research Conference (IPR'94), San Francisco, California, February 17–19, 1994. See IPR'94 Technical Digest, Vol. 3, (Optical Society of America, Washington, D.C., 1994), pp. 316–318.

4. "Communication with quantum-optic devices," presented at SPIE's international symposium, OE/LASE'94, on Technologies for Optical Fiber Communications: Optical Amplifiers for High-Speed Applications, Los Angeles, CA, 22–29 January 1994, paper 2149-07.

5. "Dispersion compensation with phase-sensitive amplifiers," (with R.-D. Li, W. L. Kath, and J. N. Kutz), presented at the 1993 Optical Society of America Annual Meeting, Toronto, Canada, October 3–8, 1993. See OSA Annual Meeting, 1993 Technical Digest Series, Vol. 16, (Optical Society of America, Washington, D.C. 1993), pp. 100.

6. "Long-Distance Pulse Propagation in Nonlinear Optical Fibers using Periodiacally-Spaced Parametric Amplifiers," (with J. N. Kutz, W. L. Kath, and R.-D. Li), presented at the Quantum Electronics and Laser Science Conference, Baltimore, Maryland, May 2-7, 1993. See Conference on Quantum Electronics and Laser Science, 1993 Technical Digest Series, Vol. 12 (Optical Society of America, Washington, D.C. 1993), pp. 289.

7. "Stable Long-Distance Pulse Propagation in Nonlinear Optical Fibers using Periodiacally Spaced Parametric Amplifiers," (with J. N. Kutz, W. L. Kath, and R.-D. Li), presented at the Integrated Photonics Research Topical Meeting (IPR'93), Palm Springs, California, March 22-24, 1993. See *Integrated Photonics Research Technical Digest, 1993* (Optical Society of America, Washington, D.C., 1993), Vol. 10, pp. 48-50.

8. R. P. Espindola, D. Y. Chu, S. L. Wu, M. K. Udo, S. T. Ho R. Tiberio, P. Chapman, H. Q. Hou, and T. Y. Chang, "Broadband Bragg Reflector in Nonlinear Semiconductor

Optical Waveguides for Soliton and WDM Applications," presented at the 1994 Optical Society of America Annual Meeting, Dallas, Texas, October 2–7, 1994. See Technical Digest, TuK2, pp. 89, October 1994.

9. X. L. Zhang, R. P. Espindola, S. L. Wu, M. K. Udo, and S. T. Ho, "Squeezed-state Generation in a Nonlinear Semiconductor Waveguide Using Delayed Pump Pulse Technique," presented at the 1994 Optical Society of America Annual Meeting, Dallas, Texas, October 2–7, 1994. See Technical Digest, WM5, pp. 119, October 1994.

10. M. K. Udo, X. L. Zhang, and S. T. Ho, " Theoretical and experimental investigations of squeezed-state generation in $\chi^{(3)}$ semiconductor waveguides," presented at the International Quantum Electronics Conference, Anaheim, California, May 8-13, 1994. See International Quantum Electronics Conference, 1994 Technical Digest Series, Vol. 9 (Optical Society of America, Washington, D.C. 1994), pp. 203.

11. Shengli Wu, Rolando P. Espindola, Maria K. Udo, W. G. Bi, Charles W. Tu, and Seng-Tiong Ho, "$Al_xGa_{1-x}P$ Waveguides with Unusually Smooth Side Walls for Nonlinear Optical Applications," presented at 1994 Conference on Lasers and Electro-optics, Anaheim, California, May 8-13, 1994. See Conference on Lasers and Electro-Optics, 1993.

12. Seng-Tiong Ho and Horace P. Yuen, "Realization of Photon Number Amplifiers," presented at 1993 Optical Society of America Annual Meeting, Toronto, Canada, October 3-8, 1993. See OSA Annual Meeting Technical Digest, 1993 (Optical Society of America, Washington, D.C., 1993), Vol. 16, pp. 69.

13. Xiaolong Zhang, Maria K. Udo, and S. T. Ho, "Improved Squeezing in Multilayer Semiconductor GaAs-AlAs Waveguides with Third-Order Nonlinearity," presented at 1993 Optical Society of America Annual Meeting, Toronto, Canada, October 3-8, 1993. See OSA Annual Meeting Technical Digest, 1993 (Optical Society of America, Washington, D.C., 1993), Vol. 16, pp. 143.

14. Sangjae Lee and S. T. Ho, "Transmission of Coupled-gap Solitons in Nonlinear Periodic Medium," presented at 1993 Optical Society of America Annual Meeting, Toronto, Canada, October 3-8, 1993. See OSA Annual Meeting Technical Digest, 1993 (Optical Society of America, Washington, D.C., 1993), Vol. 16, pp. 73.

DISTRIBUTION LIST

| addressee | number of copies |
|---|---|
| ROME LABORATORY/OCPC<br>ATTN: PAUL REPAK<br>25 ELECTRONIC PKY<br>GRIFFISS AFB NY 13441-4515 | 5 |
| NORTHWESTERN UNIVERSITY<br>ATTN: HORACE P. YUEN<br>DEPT OF ELECTRICAL ENGINEERING<br>EVANSTON IL 60208-3118 | 5 |
| RL/SUL<br>TECHNICAL LIBRARY<br>26 ELECTRONIC PKY<br>GRIFFISS AFB NY 13441-4514 | 1 |
| ADMINISTRATOR<br>DEFENSE TECHNICAL INFO CENTER<br>DTIC-FDAC<br>CAMERON STATION BUILDING 5<br>ALEXANDRIA VA 22304-6145 | 2 |
| NAVAL WARFARE ASSESSMENT CENTER<br>CODE (QA50)<br>ATTN: RAYMOND TADROS<br>PO BOX 8000<br>CORONA CA 91718-8000 | 1 |
| PHILLIPS LAB/WSR<br>ATTN: DR. CARL E. BAUM<br>3550 ABERDEEN SE<br>ALBUQUERQUE NM 87117-5776 | 1 |
| WRIGHT LABORATORY/AAAI-2, BLDG 635<br>2185 AVIONICS CIRCLE<br>WRIGHT-PATTERSON AFB OH 45433-7301 | 1 |
| AFIT ACADEMIC LIBRARY/LDEE<br>2950 P STREET<br>AREA B, BLDG 642<br>WRIGHT-PATTERSON AFB OH 45433-7765 | 1 |
| WRIGHT LABORATORY/MLPO<br>ATTN: R. L. DENISON<br>BLDG 651<br>3005 P STREET, STE 6<br>WRIGHT-PATTERSON AFB OH 45433-7707 | 1 |
| WRIGHT LABORATORY/MTE, BLDG 653<br>2977 P STREET, STE 6<br>WRIGHT-PATTERSON AFB OH 45433-7739 | 1 |

AL/CFHI, BLDG 248 1
ATTN: GILBERT G. KUPERMAN
2255 H STREET
WRIGHT-PATTERSON AFB OH 45433-7022

AIR FORCE HUMAN RESOURCES LAB 1
TECHNICAL DOCUMENTS CENTER
OL AL HSC/HRG, BLDG 190
WRIGHT-PATTERSON AFB OH 45433-7604

AUL/LSE 1
BLDG 1405
600 CHENNAULT CIRCLE
MAXWELL AFB AL 361126424

US ARMY SPACE & STRATEGIC 1
DEFENSE COMMAND
CSSD-IM-PA
PO BOX 1500
HUNTSVILLE AL 35807-3801

NAVAL AIR WARFARE CENTER 1
6000 E. 21ST STREET
INDIANAPOLIS IN 46219-2189

COMMANDING OFFICER 1
ATTN: W. BRATT
CODE 772, NCCOSC RDTE DIVISION
53560 HULL STREET
SAN DIEGO CA 92152-5001

COMMANDER, TECHNICAL LIBRARY 1
474700D/C0223
NAVAIRWARCENWPNDIV
1 ADMINISTRATION CIRCLE
CHINA LAKE CA 93555-6001

SPACE & NAVAL WARFARE SYSTEMS 2
COMMAND (PMW 178-1)
2451 CRYSTAL DRIVE
ARLINGTON VA 22245-5200

SPACE & NAVAL WARFARE SYSTEMS 1
COMMAND, EXECUTIVE DIRECTOR (PD80A)
ATTN: MR. CARL ANDRIANI
2451 CRYSTAL DRIVE
ARLINGTON VA 22245-5200

COMMANDER, SPACE & NAVAL WARFARE 1
SYSTEMS COMMAND (CODE 32)
2451 CRYSTAL DRIVE
ARLINGTON VA 22245-5200

US ARMY MISSILE COMMAND 2
AMSMI-RD-CS-R/DOCUMENTS
RSIC BLDG 4484
REDSTONE ARSENAL AL 35898-5241

ADVISORY GROUP ON ELECTRON DEVICES 1
1745 JEFFERSON DAVIS HWY
SUITE 500
ARLINGTON VA 22202

LOS ALAMOS NATIONAL LABORATORY 1
PO BOX 1663
REPORT LIBRARY, P364
LOS ALAMOS NM 87545

AEDC LIBRARY 1
TECHNICAL REPORTS FILE
100 KINDEL DRIVE, SUITE C211
ARNOLD AFB TN 37389-3211

COMMANDER 1
USAISC
ASHC-IMD-L, BLDG 61801
FT HUACHUCA AZ 85613-5000

US DEPT OF TRANSPORTATION LIBRARY 1
FB10A, M-457, RM 930
800 INDEPENDENCE AVE, SW
WASH DC 22591

AIR WEATHER SERVICE TECHNICAL 1
LIBRARY (FL 4414)
859 BUCHANAN STREET
SCOTT AFB IL 62225-5118

AFIWC/MSO 1
102 HALL BLVD, STE 315
SAN ANTONIO TX 78243-7016

DIRNSA 1
R509
9800 SAVAGE ROAD
FT MEADE MD 20755-6000

NSA/CSS 1
K1
FT MEADE MD 20755-6000

DCMAO/WICHITA/GKEP
SUITE B-34
401 N MARKET STREET
WICHITA KS 67202-2095

1

PHILLIPS LABORATORY
PL/TL (LIBRARY)
5 WRIGHT STREET
HANSCOM AFB MA 01731-3004

1

THE MITRE CORPORATION
ATTN: E. LADURE
D460
202 BURLINGTON RD
BEDFORD MA 01732

1

OUSD(P)/OTSA/DUTD
ATTN: PATRICK G. SULLIVAN, JR.
400 ARMY NAVY DRIVE
SUITE 300
ARLINGTON VA 22202

2

ATTN: DAVID D. CURTIS
ROME LABORATORY/ERAA
HANSCOM AFB, MA 01731-5000

1

ATTN: RICHARD PAYNE
ROME LABORATORY/ERD
HANSCOM AFB, MA 01731-5000

1

ATTN: JOSEPH P. LORENZO, JR.
ROME LABORATORY/EROC
HANSCOM AFB, MA 01731-5000

1

ATTN: JOSEPH L. HORNER
ROME LABORATORY/EROP
HANSCOM AFB, MA 01731-5000

1

ATTN: RICHARD A. SOREF
ROME LABORATORY/EROC
HANSCOM AFB, MA 01731-5000

1

ATTN: JOHN J. LARKIN 1
ROME LABORATORY/ERXE
HANSCOM AFB, MA 01731-5000

ATTN: DANIEL J. BURNS 1
ROME LABORATORY/ERDD
525 BROOKS RD
GRIFFISS AFB NY 13441-4505

ATTN: ALBERT A. JAMBERDINO 1
ROME LABORATORY/IRAP
32 HANGAR RD
GRIFFISS AFB NY 13441-4114

ATTN: BRIAN M. HENDRICKSON 1
ROME LABORATORY/OCP
25 ELECTRONIC PKY
GRIFFISS AFB NY 13441-4515

ATTN: GREGORY J. ZAGAR 1
ROME LABORATORY/OCPC
25 ELECTRONIC PKY
GRIFFISS AFB NY 13441-4515

ATTN: ROBERT L. KAMINSKI 1
ROME LABORATORY/C3BC
525 BROOKS RD
GRIFFISS AFB NY 13441-4505

ATTN: JAMES W. CUSACK 1
ROME LABORATORY/OCP
25 ELECTRONIC PKY
GRIFFISS AFB NY 13441-4515

ATTN: JOANNE L. ROSSI 1
ROME LABORATORY/OCP
25 ELECTRONIC PKY
GRIFFISS AFB NY 13441-4515

ATTN: ANDREW R. PIRICH 1
ROME LABORATORY/OCPA
25 ELECTRONIC PKY
GRIFFISS AFB NY 13441-4515

ATTN: RICHARD J. MICHALAK 1
ROME LABORATORY/OCPB
25 ELECTRONIC PKY
GRIFFISS AFB NY 13441-4515

NY PHOTONIC DEVELOPMENT CORP
MVCC ROME CAMPUS
UPPER FLOYD AVE
ROME, NY 13440

1

Rome Laboratory

Customer Satisfaction Survey

RL-TR-_____

Please complete this survey, and mail to RL/IMPS, 26 Electronic Pky, Griffiss AFB NY 13441-4514. Your assessment and feedback regarding this technical report will allow Rome Laboratory to have a vehicle to continuously improve our methods of research, publication, and customer satisfaction. Your assistance is greatly appreciated.
Thank You

_____

_____

Organization Name:_____(Optional)

Organization POC: _____(Optional)

Address:_____

1. On a scale of 1 to 5 how would you rate the technology developed under this research?

5-Extremely Useful 1-Not Useful/Wasteful

Rating_____

Please use the space below to comment on your rating. Please suggest improvements. Use the back of this sheet if necessary.

2. Do any specific areas of the report stand out as exceptional?

Yes___ No_____

If yes, please identify the area(s), and comment on what aspects make them "stand out."

3. Do any specific areas of the report stand out as inferior?

Yes___ No___

If yes, please identify the area(s), and comment on what aspects make them "stand out."

4. Please utilize the space below to comment on any other aspects of the report. Comments on both technical content and reporting format are desired.

☆U.S. GOVERNMENT PRINTING OFFICE: 1995-610-126-20044

# *MISSION*

# *OF*

# *ROME LABORATORY*

Mission. The mission of Rome Laboratory is to advance the science and technologies of command, control, communications and intelligence and to transition them into systems to meet customer needs. To achieve this, Rome Lab:

a. Conducts vigorous research, development and test programs in all applicable technologies;

b. Transitions technology to current and future systems to improve operational capability, readiness, and supportability;

c. Provides a full range of technical support to Air Force Materiel Command product centers and other Air Force organizations;

d. Promotes transfer of technology to the private sector;

e. Maintains leading edge technological expertise in the areas of surveillance, communications, command and control, intelligence, reliability science, electro-magnetic technology, photonics, signal processing, and computational science.

The thrust areas of technical competence include: Surveillance, Communications, Command and Control, Intelligence, Signal Processing, Computer Science and Technology, Electromagnetic Technology, Photonics and Reliability Sciences.